



The Nonlinear Viscoelastic Response of Suspensions of Vacuous Bubbles in Rubber: I — Gaussian Rubber with Constant Viscosity

Bhavesh Shrimali¹ · Kamalendu Ghosh¹ · Oscar Lopez-Pamies^{1,2} 

Received: 14 August 2021 / Accepted: 24 October 2021 / Published online: 30 November 2021
© The Author(s), under exclusive licence to Springer Nature B.V. 2021

Abstract

This paper presents an analytical and numerical study of the homogenization problem of suspensions of vacuous bubbles in viscoelastic rubber subject to finite quasistatic deformations. The focus is on the elementary case of bubbles that are initially equiaxed in shape and isotropically distributed in space and on isotropic incompressible rubber with Gaussian elasticity and constant viscosity. From an analytical point of view, asymptotic solutions are worked out in the limits: *i*) of small deformations, *ii*) of finite deformations that are applied either infinitesimally slowly or infinitely fast, and *iii*) when the rubber loses its ability to store elastic energy and reduces to a Newtonian fluid. From a numerical point of view, making use of a recently developed scheme based on a conforming Crouzeix–Raviart finite-element discretization of space and a high-order accurate explicit Runge–Kutta discretization of time, sample solutions are worked out for suspensions of initially spherical bubbles of the same (monodisperse) size under a variety of loading conditions. Consistent with a recent conjecture of Ghosh et al. (J. Mech. Phys. Solids 155:104544, 2021), the various asymptotic and numerical solutions indicate that the viscoelastic response of the suspensions features the same type of short-range-memory behavior — in contrast with the generally expected long-range-memory behavior — as that of the underlying rubber, with the distinctive differences that their effective elasticity is compressible and their effective viscosity is compressible and nonlinear. By the same token, the various solutions reveal a simple yet accurate analytical approximation for the macroscopic viscoelastic response of the suspensions under arbitrary finite quasistatic deformations.

Keywords Elastomers · Pores · Finite deformation · Internal Variables · Homogenization

✉ O. Lopez-Pamies
pamies@illinois.edu

B. Shrimali
bshrima2@illinois.edu

K. Ghosh
kg5@illinois.edu

¹ Department of Civil and Environmental Engineering, University of Illinois, Urbana–Champaign, IL 61801-2352, USA

² Département de Mécanique, École Polytechnique, 91128 Palaiseau, France

Mathematics Subject Classification 74B20 · 74Q05 · 74S05 · 76A10 · 76T20

1 Introduction

This paper is the second in a series started in [1] aimed at the study of a fundamental problem in mechanics that, in spite of its ever-increasing practical relevance, has remained *terra incognita*: the homogenization of nonlinear viscoelastic composite materials undergoing finite quasistatic deformations. Whereas the work in [1] focused on isotropic suspensions of rigid inclusions in isotropic incompressible rubber featuring Gaussian elasticity and constant viscosity, the work here focuses on isotropic suspensions of vacuous bubbles in the same elementary type of rubber. Much like in [1], attention is also restricted to equiaxed bubbles, that is, bubbles that initially are roughly spherical in shape but not necessarily smooth or without a slightly preferred direction.

The organization of the paper is as follows. After formulating the pertinent homogenization problem in Sect. 2, we devote Sects. 3 through 5 to working out analytical solutions in several asymptotic limits of physical significance. Specifically, Sect. 3 is devoted to the limit of small deformations, Sect. 4 to the limit of finite deformations that are applied either infinitesimally slowly or “infinitely” fast, and Sect. 5 to the limit when the underlying rubber matrix does not store elastic energy and reduces to a Newtonian fluid. In Sect. 6, we make use of the scheme recently introduced in [1] to generate numerical solutions for suspensions of initially spherical bubbles of monodisperse size under a variety of loading conditions suitably selected so as to reveal the defining attributes of the macroscopic response of such suspensions. With direct guidance from the asymptotic solutions in Sects. 3 through 5 and the computational solutions in Sect. 6, we propose in Sect. 7 a general analytical approximate solution for arbitrary finite quasistatic deformations. We close in Sect. 8 by summarizing and putting into perspective the results presented throughout the paper.

2 The Problem

2.1 Microscopic or Local Description of the Suspensions

Initial Configuration and Kinematics Consider a body made of bubbles embedded in a rubber matrix that in its initial configuration, at time $t = 0$, occupies the open domain $\Omega_0 \subset \mathbb{R}^3$, with boundary $\partial\Omega_0$. Denote by $\Omega_0^{(m)}$ the subdomain occupied by the matrix and by $\Omega_0^{(b)} = \Omega_0 \setminus \Omega_0^{(m)}$ that occupied collectively by the bubbles. We identify material points in the body by their initial position vector $\mathbf{X} \in \Omega_0$ and denote by $\theta_b(\mathbf{X})$ the characteristic or indicator function describing the spatial locations occupied by the bubbles in Ω_0 , that is,

$$\theta_b(\mathbf{X}) = \begin{cases} 1 & \text{if } \mathbf{X} \in \Omega_0^{(b)} \\ 0 & \text{otherwise.} \end{cases} \quad (1)$$

For later use, we also introduce the notation

$$f_0 := \frac{1}{|\Omega_0|} \int_{\Omega_0} \theta_b(\mathbf{X}) d\mathbf{X} = \frac{|\Omega_0^{(b)}|}{|\Omega_0|}$$

for the initial volume fraction of bubbles in the suspension.

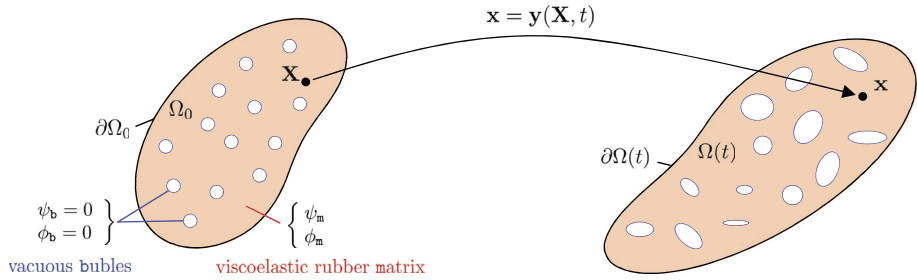


Fig. 1 Schematics of a suspension of bubbles in a viscoelastic rubber matrix in its initial undeformed configuration Ω_0 at time $t = 0$ and in a deformed configuration $\Omega(t)$ at a later time $t \in (0, T]$

In response to boundary conditions to be described below, at a time $t \in (0, T]$, the position vector \mathbf{X} of a material point may occupy a new position \mathbf{x} specified by an invertible mapping \mathbf{y} from Ω_0 to the current configuration $\Omega(t) \subset \mathbb{R}^3$. We write

$$\mathbf{x} = \mathbf{y}(\mathbf{X}, t)$$

and the associated deformation gradient and Lagrangian velocity fields at \mathbf{X} and t as

$$\mathbf{F}(\mathbf{X}, t) = \nabla \mathbf{y}(\mathbf{X}, t) = \frac{\partial \mathbf{y}}{\partial \mathbf{X}}(\mathbf{X}, t) \quad \text{and} \quad \mathbf{V}(\mathbf{X}, t) = \dot{\mathbf{y}}(\mathbf{X}, t) = \frac{\partial \mathbf{y}}{\partial t}(\mathbf{X}, t).$$

Throughout, we shall use the “dot” notation to denote the material time derivative (i.e., with \mathbf{X} held fixed) of field quantities. Figure 1 presents a schematic of the body under consideration in its initial undeformed configuration Ω_0 at time $t = 0$ and in an arbitrary deformed configuration $\Omega(t)$ at a later time $t \in (0, T]$.

Constitutive Behavior of the Rubber The focus of this paper is on the basic case of viscoelastic rubber with *Gaussian elasticity* and *constant viscosity* under isothermal conditions. Precisely, making use of the powerful two-potential formalism [2–4], the constitutive behavior of the rubber is expediently characterized by the two thermodynamic potentials

$$\psi_m(\mathbf{F}, \mathbf{F}^v) = \begin{cases} \underbrace{\frac{\mu_m}{2} [I_1 - 3]}_{\psi_m^{\text{Eq}}(\mathbf{F})} + \underbrace{\frac{\nu_m}{2} [I_1^e - 3]}_{\psi_m^{\text{NEq}}(\mathbf{F}\mathbf{F}^{v-1})} & \text{if } J = 1 \\ +\infty & \text{otherwise} \end{cases} \quad (2)$$

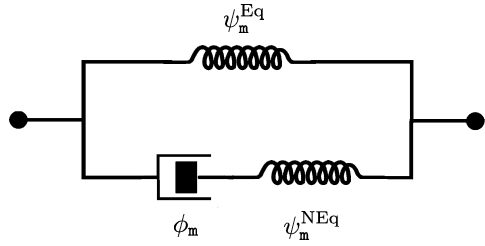
and

$$\phi_m(\mathbf{F}, \mathbf{F}^v, \dot{\mathbf{F}}^v) = \begin{cases} \frac{1}{2} \dot{\mathbf{F}}^v \mathbf{F}^{v-1} \cdot [2 \eta_m \mathcal{K} \dot{\mathbf{F}}^v \mathbf{F}^{v-1}] & \text{if } \text{tr}(\dot{\mathbf{F}}^v \mathbf{F}^{v-1}) = 0 \\ +\infty & \text{otherwise,} \end{cases} \quad (3)$$

where ψ_m and ϕ_m stand, respectively, for the free energy and dissipation potential describing how the rubber stores and dissipates energy through elastic and viscous deformation. In these expressions, the second-order tensor \mathbf{F}^v is an internal variable of state that describes roughly the “viscous part” of the deformation gradient \mathbf{F} ,

$$I_1 = \mathbf{F} \cdot \mathbf{F} = \text{tr } \mathbf{C}, \quad J = \det \mathbf{F} = \sqrt{\det \mathbf{C}}, \quad I_1^e = \mathbf{F}\mathbf{F}^{v-1} \cdot \mathbf{F}\mathbf{F}^{v-1} = \text{tr}(\mathbf{C}\mathbf{C}^{v-1}),$$

Fig. 2 Rheological representation of rubber



where $\mathbf{C} = \mathbf{F}^T \mathbf{F}$ denotes the right Cauchy-Green deformation tensor, $\mathbf{C}^v = \mathbf{F}^{vT} \mathbf{F}^v$,

$$\mathcal{K}_{ijkl} = \frac{1}{2} \left(\delta_{ik} \delta_{jl} + \delta_{il} \delta_{jk} - \frac{2}{3} \delta_{ij} \delta_{kl} \right) \tag{4}$$

stands for the (components¹ of the) standard deviatoric orthogonal projection tensor, the usual notation $(\mathcal{K} \mathbf{F}^v \mathbf{F}^{v-1})_{ij} = \mathcal{K}_{ijkl} \dot{F}_{kp}^v F_{pl}^{v-1}$ for a fourth-order tensor acting on a second-order tensor is employed, and $\mu_m \geq 0, \nu_m \geq 0, \eta_m \geq 0$ are material constants.

The interested reader is referred to [4] for a complete account of the two-potential framework as it pertains to rubber. Here, we merely recall that the model (2)–(3) can be thought of as the classical Zener or standard solid model [5] suitably generalized to account for the constitutive and geometric nonlinearities inherent to the setting of finite deformations. More specifically, as schematically depicted by the rheological representation in Fig. 2, the function ψ_m^{Eq} in (2) characterizes the Gaussian elastic energy storage in the rubber at states of thermodynamic equilibrium, whereas ψ_m^{NEq} characterizes the additional Gaussian elastic energy storage at non-equilibrium states (i.e., the part of the energy that gets dissipated eventually). On the other hand, the parameter η_m in (3) characterizes the constant viscosity of the rubber.

Constitutive Behavior of the Bubbles Furthermore, the focus is on the equally basic class of *vacuous* bubbles. Such a limiting constitutive behavior can also be conveniently cast within the two-potential formalism. In this case, the free energy and dissipation potential read trivially as

$$\psi_b = 0 \quad \text{and} \quad \phi_b = 0. \tag{5}$$

Pointwise Constitutive Behavior of the Suspension Given the characteristic function (1) for the bubbles and the free energies (2), (5)₁ and dissipation potentials (3), (5)₂ for the rubber and the bubbles, the pointwise free energy and dissipation potential for the suspension can be compactly written as

$$\psi(\mathbf{X}, \mathbf{F}, \mathbf{F}^v) = (1 - \theta_b(\mathbf{X})) \psi_m(\mathbf{F}, \mathbf{F}^v) \quad \text{and} \quad \phi(\mathbf{X}, \mathbf{F}, \mathbf{F}^v, \dot{\mathbf{F}}^v) = (1 - \theta_b(\mathbf{X})) \phi_m(\mathbf{F}, \mathbf{F}^v, \dot{\mathbf{F}}^v).$$

It then follows that the first Piola-Kirchhoff stress tensor \mathbf{S} at any material point $\mathbf{X} \in \Omega_0$ and time $t \in [0, T]$ reads

$$\mathbf{S}(\mathbf{X}, t) = \frac{\partial \psi}{\partial \mathbf{F}}(\mathbf{X}, \mathbf{F}, \mathbf{F}^v), \tag{6}$$

¹Throughout, the components of all tensorial quantities are referred to the laboratory Cartesian frame of reference $\{e_i\}$ $i = 1, 2, 3$ and the summation convention is employed.

where \mathbf{F}^v is implicitly defined by the evolution equation

$$\begin{cases} \frac{\partial \psi}{\partial \mathbf{F}^v}(\mathbf{X}, \mathbf{F}, \mathbf{F}^v) + \frac{\partial \phi}{\partial \dot{\mathbf{F}}^v}(\mathbf{X}, \mathbf{F}, \mathbf{F}^v, \dot{\mathbf{F}}^v) = \mathbf{0} \\ \mathbf{F}^v(\mathbf{X}, 0) = \mathbf{I}. \end{cases} \tag{7}$$

Upon direct use of the expressions (2), (3), (5) and some algebraic manipulation, it further follows that the pointwise constitutive response (6)–(7) of the suspension takes the more explicit form

$$\mathbf{S}(\mathbf{X}, t) = (1 - \theta_b(\mathbf{X})) [\mu_m \mathbf{F} - p \mathbf{F}^{-T} + \nu_m \mathbf{F} \mathbf{C}^{v-1}], \tag{8}$$

where p is the arbitrary hydrostatic pressure associated with the incompressibility constraint of the rubber matrix and \mathbf{C}^v is defined by the evolution equation

$$\begin{cases} \dot{\mathbf{C}}^v(\mathbf{X}, t) = \frac{\nu_m}{\eta_m} \left[\mathbf{C} - \frac{1}{3} (\mathbf{C} \cdot \mathbf{C}^{v-1}) \mathbf{C}^v \right] \\ \mathbf{C}^v(\mathbf{X}, 0) = \mathbf{I}. \end{cases} \tag{9}$$

Here, it is important to note that the dependence on the internal variable \mathbf{F}^v enters (8) and (9) only through the symmetric combination $\mathbf{C}^v = \mathbf{F}^{vT} \mathbf{F}^v$.

Remark 1 The pointwise constitutive behavior (8)–(9) contains two important limiting cases. The first one, which corresponds to setting the rubber viscosity either to $\eta_m = 0$ or $\eta_m \rightarrow +\infty$, is that of a suspension of bubbles in a *Gaussian elastic solid*. The second one, which corresponds to setting the equilibrium and non-equilibrium rubber moduli to $\mu_m = 0$ and $\nu_m \rightarrow +\infty$, is that of a suspension of bubbles in a *Newtonian fluid*.

To see the specialization to the elastic solid limiting case, note that when $\eta_m = 0$, the solution to the evolution equation (9) is simply $\mathbf{C}^v = \mathbf{C}$ and the first Piola-Kirchhoff stress tensor (8) reduces, with a slight abuse of notation, to $\mathbf{S}(\mathbf{X}, t) = (1 - \theta_b(\mathbf{X})) [\mu_m \mathbf{F} - p \mathbf{F}^{-T}]$. Similarly, when $\eta_m \rightarrow +\infty$, the solution to the evolution equation (9) is $\mathbf{C}^v = \mathbf{I} + O(\eta_m^{-1})$ and the first Piola-Kirchhoff stress tensor (8) reduces to $\mathbf{S}(\mathbf{X}, t) = (1 - \theta_b(\mathbf{X})) [(\mu_m + \nu_m) \mathbf{F} - p \mathbf{F}^{-T}]$.

On the other hand, to see the specialization to the viscous fluid limiting case, note that when $\mu_m = 0$ and $\nu_m \rightarrow +\infty$, the solution to the evolution equation (9) is given $\mathbf{C}^v = \mathbf{C} + \nu_m^{-1} (-\eta_m \dot{\mathbf{C}} + p_1 \mathbf{C}) + O(\nu_m^{-2})$ and the first Piola-Kirchhoff stress tensor (8) reduces to $\mathbf{S}(\mathbf{X}, t) = (1 - \theta_b(\mathbf{X})) [\eta_m (\mathbf{F} \mathbf{F}^{-1} \mathbf{F}^{-T} + \mathbf{F}^{-T} \dot{\mathbf{F}}^T \mathbf{F}^{-T}) - q \mathbf{F}^{-T}]$; in these last two expressions, p_1 and q are arbitrary hydrostatic pressures associated with the incompressibility constraint of the rubber matrix. Accordingly, the Cauchy stress tensor $\mathbf{T} = \mathbf{S} \mathbf{F}^T$ specializes to $\mathbf{T}(\mathbf{x}, t) = (1 - \chi_b(\mathbf{x})) [2\eta_m \mathbf{D} - q \mathbf{I}]$, where $\mathbf{D} = 1/2 (\dot{\mathbf{F}} \mathbf{F}^{-1} + \mathbf{F}^{-T} \dot{\mathbf{F}}^T)$ is the rate of deformation tensor and $\chi_b(\mathbf{y}(\mathbf{X}, t)) = \theta_b(\mathbf{X})$ is the characteristic function describing the spatial locations occupied by the bubbles in the deformed configuration $\Omega(t)$.

2.2 Macroscopic or Homogenized Response

In the sequel, we wish to restrict attention to suspensions when initially, at time $t = 0$, the bubbles are distributed isotropically throughout the rubber and are of equiaxed shape and of much smaller size than the size of the body. Such suspensions are expected to behave macroscopically as homogeneous isotropic materials. Their macroscopic or homogenized

response can be defined as the relation between the history of the volume average of the first Piola-Kirchhoff stress

$$\{\mathbf{S}(t), t \in [0, T]\}, \quad \mathbf{S}(t) := \frac{1}{|\Omega_0|} \int_{\Omega_0} \mathbf{S}(\mathbf{X}, t) \, d\mathbf{X} \tag{10}$$

and the history of the volume average of the deformation gradient

$$\{\mathbf{F}(t), t \in [0, T]\}, \quad \mathbf{F}(t) := \frac{1}{|\Omega_0|} \int_{\Omega_0} \mathbf{F}(\mathbf{X}, t) \, d\mathbf{X} \tag{11}$$

when they are subjected to affine boundary conditions [6, 7].

For affine deformations, when $\mathbf{F}(t)$ is prescribed, the problem amounts to solving the initial-boundary-value problem

$$\begin{cases} \text{Div} [(1 - \theta_b(\mathbf{X})) (\mu_m \nabla \mathbf{y} - p \nabla \mathbf{y}^{-T} + \nu_m \nabla \mathbf{y} \mathbf{C}^{v-1})] = \mathbf{0}, & (\mathbf{X}, t) \in \Omega_0 \times [0, T] \\ \det \nabla \mathbf{y} = 1, & (\mathbf{X}, t) \in \Omega_0^{(m)} \times [0, T] \\ \mathbf{y}(\mathbf{X}, t) = \mathbf{F}(t)\mathbf{X}, & (\mathbf{X}, t) \in \partial\Omega_0 \times [0, T] \\ \mathbf{y}(\mathbf{X}, 0) = \mathbf{X}, & \mathbf{X} \in \Omega_0 \end{cases} \tag{12}$$

coupled with the evolution equation

$$\begin{cases} \dot{\mathbf{C}}^v(\mathbf{X}, t) = \frac{\nu_m}{\eta_m} \left[\nabla \mathbf{y}^T \nabla \mathbf{y} - \frac{1}{3} (\nabla \mathbf{y}^T \nabla \mathbf{y} \cdot \mathbf{C}^{v-1}) \mathbf{C}^v \right], & (\mathbf{X}, t) \in \Omega_0^{(m)} \times [0, T] \\ \mathbf{C}^v(\mathbf{X}, 0) = \mathbf{I}, & \mathbf{X} \in \Omega_0^{(m)} \end{cases} \tag{13}$$

for the deformation field $\mathbf{y}(\mathbf{X}, t)$, the pressure field $p(\mathbf{X}, t)$, and the internal variable $\mathbf{C}^v(\mathbf{X}, t)$, and then computing the resulting history of the macroscopic stress (10).

It is worth noting that equation (12)₁ is nothing more than balance of linear momentum, $\text{Div} \mathbf{S} = \mathbf{0}$, specialized to the constitutive behavior (8) in the absence of inertia and body forces. By virtue of the material frame indifference of the thermodynamic potentials (2), (3), and (5), balance of angular momentum, $\mathbf{S}\mathbf{F}^T = \mathbf{F}\mathbf{S}^T$, is automatically satisfied; see Sect. 2.1 in [4]. Withal, the nonlinear initial-boundary-value problem (12)–(13) does not generally admit analytical solutions and hence must be solved numerically. In a recent contribution, as alluded to above, Ghosh et al. [1] have introduced a robust scheme based on a finite-element (FE) discretization of space and a finite-difference discretization of time for such a class of problems. In Sect. 6 below, we make use of this scheme to generate numerical solutions to (12)–(13) for suspensions of initially spherical bubbles of monodisperse size under a variety of loading conditions. Preceding those, in Sects. 3, 4, 5, we work out insightful asymptotic solutions in several limits of physical significance that allow for analytical treatment, namely, the limits of: (i) small deformations, (ii) finite deformations for slow and fast deformation rates, and (iii) finite deformations in the absence of storage of elastic energy when the rubber reduces to a Newtonian fluid.

3 The Homogenized Response in the Small-Deformation Limit

As anticipated above, one of a handful of limiting regimes in which the macroscopic response of the suspension of bubbles can be worked out analytically is that of small deformations when $\|\mathbf{F}(t) - \mathbf{I}\| \rightarrow 0$. In such a limit, the nonlinear viscoelasticity problem (12)–(13)

reduces asymptotically to one of linear viscoelasticity that can be solved in terms of a *single linear elastostatics* problem. The calculations go as follows.

As a first step, introduce the macroscopic deformation measure $\mathbf{H}(t) = \mathbf{F}(t) - \mathbf{I}$ together with the ansatz

$$\begin{aligned} \mathbf{y}(\mathbf{X}, t) &= \mathbf{X} + \mathbf{u}(\mathbf{X}, t) + O(\|\mathbf{H}(t)\|^2) \quad \text{with} \quad u_i(\mathbf{X}, t) = \Gamma_{ijk}(\mathbf{X}, t)H_{jk}(t), \\ p(\mathbf{X}, t) &= \mu_m + \nu_m + p_0(\mathbf{X}, t) + O(\|\mathbf{H}(t)\|^2) \quad \text{with} \quad p_0(\mathbf{X}, t) = \Sigma_{jk}(\mathbf{X}, t)H_{jk}(t), \\ \mathbf{C}^v(\mathbf{X}, t) &= \mathbf{I} + \mathbf{H}^v(\mathbf{X}, t) + \mathbf{H}^{vT}(\mathbf{X}, t) + O(\|\mathbf{H}(t)\|^2) \quad \text{with} \quad H_{ij}^v(\mathbf{X}, t) = \Upsilon_{ijkl}(\mathbf{X}, t)H_{kl}(t) \end{aligned} \tag{14}$$

for the solution to (12)–(13) in the limit as $\|\mathbf{H}(t)\| \rightarrow 0$. Note that the tensors $\mathbf{\Gamma}$, $\mathbf{\Sigma}$, $\mathbf{\Upsilon}$ are concentration tensors quantifying the linearity of the fields in the applied boundary data $\mathbf{H}(t)$.

On substitution of (14), to leading $O(\|\mathbf{H}(t)\|)$, the governing equations (12)–(13) reduce to the initial-boundary-value problem

$$\left\{ \begin{aligned} &\text{Div} \left[(1 - \theta_b(\mathbf{X})) (\mu_m(\nabla \mathbf{u} + \nabla \mathbf{u}^T) - p_0 \mathbf{I} + \nu_m(\nabla \mathbf{u} + \nabla \mathbf{u}^T - \mathbf{H}^v - \mathbf{H}^{vT})) \right] = \mathbf{0}, \\ &\quad (\mathbf{X}, t) \in \Omega_0 \times [0, T] \\ &\text{tr } \nabla \mathbf{u} = 0, \quad (\mathbf{X}, t) \in \Omega_0^{(m)} \times [0, T] \\ &\mathbf{u}(\mathbf{X}, t) = \mathbf{H}(t)\mathbf{X}, \quad (\mathbf{X}, t) \in \partial\Omega_0 \times [0, T] \\ &\mathbf{u}(\mathbf{X}, 0) = \mathbf{0}, \quad \mathbf{X} \in \Omega_0 \end{aligned} \right. \tag{15}$$

coupled with the evolution equation

$$\left\{ \begin{aligned} &\dot{\mathbf{H}}^v(\mathbf{X}, t) = \frac{\nu_m}{\eta_m} [\nabla \mathbf{u} - \mathbf{H}^v], \quad (\mathbf{X}, t) \in \Omega_0^{(m)} \times [0, T] \\ &\mathbf{H}^v(\mathbf{X}, 0) = \mathbf{0}, \quad \mathbf{X} \in \Omega_0^{(m)} \end{aligned} \right. \tag{16}$$

for the displacement field $\mathbf{u}(\mathbf{X}, t)$, the pressure field $p_0(\mathbf{X}, t)$, and the internal variable $\mathbf{H}^v(\mathbf{X}, t)$.

Now, the linear system of ordinary differential equations (16) admits the simple explicit solution

$$\mathbf{H}^v(\mathbf{X}, t) = \int_0^t \frac{e^{-\frac{t-\tau}{\tau_m}}}{\tau_m} \nabla \mathbf{u}(\mathbf{X}, \tau) d\tau, \quad \tau_m := \frac{\eta_m}{\nu_m}, \tag{17}$$

which prompts the introduction of the initial relaxation modulus for the suspension

$$\mathbf{L}(\mathbf{X}, t) = (1 - \theta_b(\mathbf{X})) \mathbf{L}_m(t) \quad \text{with} \quad \mathbf{L}_m(t) = 2 \left(\mu_m + \nu_m e^{-\frac{t}{\tau_m}} \right) \mathcal{K}$$

and, in turn, the rewrite of equations (15)–(16) in the compact hereditary-integral-type form

$$\left\{ \begin{aligned} &\text{Div} \left[\int_{-\infty}^t \mathbf{L}(\mathbf{X}, t - \tau) \frac{\partial \nabla \mathbf{u}}{\partial \tau}(\mathbf{X}, \tau) d\tau - (1 - \theta_b(\mathbf{X})) p_0 \mathbf{I} \right] = \mathbf{0}, \quad (\mathbf{X}, t) \in \Omega_0 \times [0, T] \\ &\text{tr } \nabla \mathbf{u} = 0, \quad (\mathbf{X}, t) \in \Omega_0^{(m)} \times [0, T] \\ &\mathbf{u}(\mathbf{X}, t) = \mathbf{H}(t)\mathbf{X}, \quad (\mathbf{X}, t) \in \partial\Omega_0 \times [0, T] \\ &\mathbf{u}(\mathbf{X}, 0) = \mathbf{0}, \quad \mathbf{X} \in \Omega_0, \end{aligned} \right. \tag{18}$$

where we recall that \mathcal{K} stands for the deviatoric orthogonal projection tensor (4) and it is tacitly assumed that $\mathbf{u}(\mathbf{X}, t) = \mathbf{0}$ for $t < 0$.

Next, applying the standard one-sided Laplace transform $\mathcal{L}\{f(t)\} = \widehat{f}(s) = \int_0^\infty f(t)e^{-st} dt$ to equations (18) yields

$$\begin{cases} \text{Div} [\widetilde{\mathbf{L}}(\mathbf{X}, s) \nabla \widehat{\mathbf{u}}(\mathbf{X}, s) - (1 - \theta_b(\mathbf{X})) \widehat{p}_0 \mathbf{I}] = \mathbf{0}, & \mathbf{X} \in \Omega_0 \\ \text{tr} \nabla \widehat{\mathbf{u}} = 0, & \mathbf{X} \in \Omega_0^{(m)} \\ \widehat{\mathbf{u}}(\mathbf{X}, s) = \widehat{\mathbf{H}}(s) \mathbf{X}, & \mathbf{X} \in \partial \Omega_0 \\ \widehat{\mathbf{u}}(\mathbf{X}, 0) = \mathbf{0}, & \mathbf{X} \in \Omega_0, \end{cases} \tag{19}$$

where

$$\widetilde{\mathbf{L}}(\mathbf{X}, s) = s \widehat{\mathbf{L}}(\mathbf{X}, s) = (1 - \theta_b(\mathbf{X})) s \widehat{\mathbf{L}}_m(s) = (1 - \theta_b(\mathbf{X})) 2 \left(\mu_m + \frac{\nu_m \tau_m s}{1 + \tau_m s} \right) \mathcal{K}.$$

Save for the parametric dependence on the Laplace variable s of the modulus $\widetilde{\mathbf{L}}(\mathbf{X}, s)$, as expected, the governing equations (19) in the Laplace domain for the fields $\widehat{\mathbf{u}}(\mathbf{X}, s)$ and $\widehat{p}_0(\mathbf{X}, s)$ are of identical mathematical structure as the governing equations for the displacement and pressure fields in a linear elastic composite material with the same two-phase microstructure as the viscoelastic suspension. What is more, the dependence on the Laplace variable s can be factored out to conclude that the displacement and pressure fields solution of (19) are of the separable form

$$\widehat{u}_i(\mathbf{X}, s) = \Gamma_{ikl}(\mathbf{X}) \widehat{H}_{kl}(s) \quad \text{and} \quad \widehat{p}_0(\mathbf{X}, s) = \Sigma_{ij}(\mathbf{X}) \widehat{H}_{ij}(s), \tag{20}$$

where the concentration tensors $\Gamma(\mathbf{X})$ and $\Sigma(\mathbf{X})$ are solution of the s -independent linear elastostatics problem

$$\begin{cases} \frac{\partial}{\partial X_j} \left[(1 - \theta_b(\mathbf{X})) \left(\mathcal{K}_{ijmn} \frac{\partial \Gamma_{mkl}}{\partial X_n}(\mathbf{X}) - \frac{1}{2} \delta_{ij} \Sigma_{kl}(\mathbf{X}) \right) \right] = 0, & \mathbf{X} \in \Omega_0 \\ \frac{\partial \Gamma_{mkl}}{\partial X_m}(\mathbf{X}) = 0, & \mathbf{X} \in \Omega_0^{(m)} \\ \Gamma_{ikl}(\mathbf{X}) = \delta_{ik} X_l, & \mathbf{X} \in \partial \Omega_0. \end{cases} \tag{21}$$

It immediately follows from the separable solution (20) with (21) in the Laplace domain that the history of the macroscopic stress (10) in the time domain is given by

$$\begin{aligned} \mathbf{s}(t) &= \int_{-\infty}^t \bar{\mathbf{L}}(t - \tau) \frac{\partial \mathbf{H}}{\partial \tau}(\tau) d\tau + O(\|\mathbf{H}\|^2) \quad \text{with} \\ \bar{\mathbf{L}}(t) &= 2 \left(\bar{\mu} + \bar{\nu} e^{-\frac{t}{\bar{\tau}_{\mathcal{K}}}} \right) \mathcal{K} + 3 \left(\bar{\kappa} + \bar{\omega} e^{-\frac{t}{\bar{\tau}_{\mathcal{J}}}} \right) \mathcal{J}, \end{aligned} \tag{22}$$

where, again, \mathcal{K} stands for the deviatoric orthogonal projection tensor (4),

$$\mathcal{J}_{ijkl} = \frac{1}{3} \delta_{ij} \delta_{kl}$$

denotes the volumetric orthogonal projection tensor, and where the six effective material constants $\bar{\mu}, \bar{\kappa}, \bar{\nu}, \bar{\omega}, \bar{\tau}_{\mathcal{K}}, \bar{\tau}_{\mathcal{J}}$ are given by the expressions

$$\bar{\mu} = g(f_0) \mu_m, \quad \bar{\kappa} = h(f_0) \mu_m, \quad \bar{\nu} = g(f_0) \nu_m, \quad \bar{\omega} = h(f_0) \nu_m, \quad \bar{\tau}_{\mathcal{K}} = \bar{\tau}_{\mathcal{J}} = \tau_m \tag{23}$$

in terms of the material constants μ_m, ν_m, η_m of the rubber matrix and the microstructural coefficients

$$\begin{aligned}
 g(f_0) &= \frac{1}{5|\Omega_0|} \int_{\Omega_0} (1 - \theta_b(\mathbf{X})) \mathcal{K}_{klmn} \frac{\partial \Gamma_{mkl}}{\partial X_n}(\mathbf{X}) d\mathbf{X} \quad \text{and} \\
 h(f_0) &= -\frac{1}{3|\Omega_0|} \int_{\Omega_0} (1 - \theta_b(\mathbf{X})) \Sigma_{kk}(\mathbf{X}) d\mathbf{X}.
 \end{aligned}
 \tag{24}$$

Remark 2 The coefficients (24) depend, of course, not just on the initial volume fraction f_0 of the bubbles but on the entire characteristic function θ_b describing their initial shape, relative size, and spatial distribution. We use f_0 as their sole argument for notational simplicity. Their computation requires the solution of the boundary-value problem (21) for the concentration tensors $\Gamma(\mathbf{X})$ and $\Sigma(\mathbf{X})$. In general, this problem is only solvable numerically; see, e.g., the Appendix in [8]. Howbeit, there are classes of suspensions of practical interest that do admit analytical solutions for (24). By making combined use of various classes of iterative techniques [9–12], as part of an analysis of the phenomenon of elastic cavitation in rubber, Lopez-Pamies et al. [13, 14] constructed one such class of suspensions for which the coefficients (24) simply read

$$g(f_0) = \frac{3(1 - f_0)}{3 + 2f_0} \quad \text{and} \quad h(f_0) = \frac{4(1 - f_0)}{3f_0}.
 \tag{25}$$

It corresponds to a suspension of bubbles of abstract shape and infinitely many sizes distributed in a manner such that they can fill the entire space, thus its percolation at $f_0 = 1$. The attentive reader will note that the results (25) coincide identically with the corresponding Hashin-Shtrikman (HS) upper bound [15]. Despite their exactness for a certain type of abstract microstructure, recent numerical solutions [16] have shown that in fact the results (25) remain accurately descriptive of isotropic suspensions of equiaxed vacuous bubbles at large, regardless of the relative sizes of the bubbles to one another, for initial volume fractions in the small-to-moderate range $f_0 \in [0, 0.30]$. In other words, the coefficients (24) are fairly insensitive to the initial (equiaxed) shape, relative size, and (isotropic) spatial distribution of the bubbles up to about $f_0 = 0.30$. In this regard and for later reference, we introduce the notation

$$\begin{aligned}
 \bar{\mu}^{HS} &= \frac{3(1 - f_0)}{3 + 2f_0} \mu_m, & \bar{\kappa}^{HS} &= \frac{4(1 - f_0)}{3f_0} \mu_m, \\
 \bar{\nu}^{HS} &= \frac{3(1 - f_0)}{3 + 2f_0} \nu_m, & \bar{\omega}^{HS} &= \frac{4(1 - f_0)}{3f_0} \nu_m
 \end{aligned}
 \tag{26}$$

for the specialization of (23)_{1–4} to suspensions for which the coefficients $g(f_0)$ and $h(f_0)$ are given by (25).

Remark 3 The macroscopic response (22) of the suspension is of the same functional form as the response of the underlying rubber matrix, namely, an isotropic Zener viscoelastic solid, albeit a *compressible* one due to the presence of the vacuous bubbles. To see this more thoroughly, note that the hereditary-integral-type relation (22) can be rewritten as the internal-variable-type relation

$$\begin{aligned}
 \mathbf{S}(t) &= 2\bar{\mu} \left[\boldsymbol{\varepsilon} - \frac{1}{3} \text{tr}(\boldsymbol{\varepsilon}) \mathbf{I} \right] + \bar{\kappa} \text{tr}(\boldsymbol{\varepsilon}) \mathbf{I} + 2\bar{\nu} \left[\boldsymbol{\varepsilon} - \boldsymbol{\varepsilon}^v - \frac{1}{3} \text{tr}(\boldsymbol{\varepsilon} - \boldsymbol{\varepsilon}^v) \mathbf{I} \right] + \\
 &\quad \bar{\omega} \text{tr}(\boldsymbol{\varepsilon} - \boldsymbol{\varepsilon}^v) \mathbf{I} + O(\|\mathbf{H}\|^2),
 \end{aligned}
 \tag{27}$$

where $\boldsymbol{\epsilon} = 1/2(\mathbf{H} + \mathbf{H}^T)$ stands for the infinitesimal strain tensor, $\boldsymbol{\epsilon}^v$ is a macroscopic internal variable defined by the evolution equation

$$\begin{cases} \dot{\boldsymbol{\epsilon}}^v(t) = \frac{\bar{\nu}}{\bar{\eta}_{\mathcal{K}}} (\boldsymbol{\epsilon} - \boldsymbol{\epsilon}^v) + \frac{1}{3} \left(\frac{\bar{\omega}}{\bar{\eta}_{\mathcal{J}}} - \frac{\bar{\nu}}{\bar{\eta}_{\mathcal{K}}} \right) \text{tr}(\boldsymbol{\epsilon} - \boldsymbol{\epsilon}^v) \mathbf{I} \\ \boldsymbol{\epsilon}^v(0) = \mathbf{0}, \end{cases} \tag{28}$$

and where

$$\bar{\eta}_{\mathcal{K}} = g(f_0)\eta_m \quad \text{and} \quad \bar{\eta}_{\mathcal{J}} = h(f_0)\eta_m \tag{29}$$

denote the initial deviatoric and volumetric effective viscosities of the suspension. Note that thanks to the equality $\bar{\omega}/\bar{\eta}_{\mathcal{J}} = \bar{\nu}/\bar{\eta}_{\mathcal{K}}$, the evolution equation (28) specializes to

$$\begin{cases} \dot{\boldsymbol{\epsilon}}^v(t) = \frac{\bar{\nu}}{\bar{\eta}_{\mathcal{K}}} (\boldsymbol{\epsilon} - \boldsymbol{\epsilon}^v) \\ \boldsymbol{\epsilon}^v(0) = \mathbf{0}, \end{cases}$$

which is the same evolution equation as (17), but free of the incompressibility constraint. Consistent with an observation of Hashin [21] and as discussed more generally in Sect. 9 of [1] and in Sect. 8 below, the reason why the homogenized response (22), or equivalently (27)–(28), for suspensions of vacuous bubbles in rubber is — contrary to the general expectation [7, 22, 23] — of the same form as that of the underlying rubber matrix can be attributed to the fact that there is *only one* relaxation mechanism in the suspensions, namely, the shear relaxation of the rubber.

4 The Homogenized Response at Finite Deformations for Slow and Fast Deformation Rates

Two other limiting regimes for which the macroscopic response of the suspension of bubbles can be worked out analytically are those when the deformation is applied either infinitesimally slowly or “infinitely” fast² in time t . In both of these cases, as spelled out next, the nonlinear viscoelasticity problem (12)–(13) reduces asymptotically to the same type of problem in *finite elastostatics*.

4.1 The Limiting Case of Infinitesimally Slow Deformations

Consider first deformations that are applied slowly. To this end, without loss of generality, take the macroscopic deformation gradient $\mathbf{F}(t)$ to be of the asymptotic form

$$\mathbf{F}(t) = \mathbf{F}_0 + t^{-1}\mathbf{F}_1 + O(t^{-2}) \tag{30}$$

in the limit as $t \rightarrow T = +\infty$. Here, \mathbf{F}_0 and \mathbf{F}_1 are constant second-order tensors of choice, the former one describing a macroscopic deformation gradient that is applied infinitesimally slowly.

²In the present context of quasistatic deformations, “infinitely” fast is meant in the usual sense of loading conditions that are applied in a time scale that is much smaller than the characteristic relaxation time of the problem (here, $\tau_m = \eta_m/\nu_m$), but still large enough that inertial effects can be neglected.

Granted (30), we look for solutions to (12)–(13) of the asymptotic form

$$\begin{aligned} \mathbf{y}(\mathbf{X}, t) &= \mathbf{y}_0(\mathbf{X}) + t^{-1}\mathbf{y}_1(\mathbf{X}) + O(t^{-2}), \\ p(\mathbf{X}, t) &= p_0(\mathbf{X}) + t^{-1}p_1(\mathbf{X}) + O(t^{-2}), \\ \mathbf{C}^v(\mathbf{X}, t) &= \mathbf{C}_0^v(\mathbf{X}) + t^{-1}\mathbf{C}_1^v(\mathbf{X}) + O(t^{-2}) \end{aligned} \tag{31}$$

in the limit as $t \rightarrow +\infty$. On substitution of (31)₃, noting that

$$\dot{\mathbf{C}}^v = -t^{-2}\mathbf{C}_1^v + O(t^{-3}) \quad \text{and} \quad \mathbf{C}^{v-1} = \mathbf{C}_0^{v-1} - t^{-1}\mathbf{C}_0^{v-1}\mathbf{C}_1^v\mathbf{C}_0^{v-1} + O(t^{-2}),$$

standard calculations suffice to solve equation (13) for the internal variable $\mathbf{C}^v(\mathbf{X}, t)$ to leading order to determine that

$$\mathbf{C}_0^v = \nabla \mathbf{y}_0^T \nabla \mathbf{y}_0.$$

In turn, on substitution of (31) alongside use of this last result, it is straightforward to deduce that, to leading order, equations (12) simplify to the boundary-value problem

$$\begin{cases} \text{Div} [(1 - \theta_b(\mathbf{X})) (\mu_m \nabla \mathbf{y}_0 - (p_0 - v_m) \nabla \mathbf{y}_0^{-T})] = \mathbf{0}, & \mathbf{X} \in \Omega_0 \\ \det \nabla \mathbf{y}_0 = 1, & \mathbf{X} \in \Omega_0^{(m)} \\ \mathbf{y}_0(\mathbf{X}) = \mathbf{F}_0 \mathbf{X}, & \mathbf{X} \in \partial \Omega_0 \end{cases} \tag{32}$$

for the deformation field $\mathbf{y}_0(\mathbf{X})$ and pressure field $p_0(\mathbf{X})$.

Equations (32) are nothing more than the governing equations for the homogenized elastic response of a random isotropic suspension of vacuous bubbles, with characteristic function θ_b , embedded in a Gaussian rubber matrix with initial shear modulus μ_m . In a recent contribution, Shrimali et al. [16] have worked out rigorous computational and analytical solutions precisely for such a homogenization problem; see [17–20] for earlier analogous results in 2D. They did so for a wide spectrum of characteristic functions θ_b , which guided them to concoct a remarkably simple yet accurate approximate solution; see Remark 6 in [16]. When applied to the problem of interest here, their result states that the macroscopic stress (10) corresponding to a macroscopic deformation gradient \mathbf{F}_0 that is applied infinitesimally slowly is accurately approximated by the formula

$$\begin{aligned} \mathbf{S}(t) &= \frac{3(1 - f_0)}{3 + 2f_0} \mu_m \mathbf{F}_0 + \frac{\mu_m}{2} \left[\frac{3 + 6J_0 + 2f_0(1 + 7J_0)}{(3 + 2f_0)J_0^{1/3}} + \frac{f_0^{1/3} J_0(4 - 5f_0 - 4J_0)}{(J_0 + f_0 - 1)^{4/3}} \right] \mathbf{F}_0^{-T} \\ &\quad + O(t^{-1}), \end{aligned} \tag{33}$$

where $J_0 = \det \mathbf{F}_0$.

4.2 The Limiting Case of “Infinitely” Fast Deformations

Consider now an applied macroscopic deformation gradient of the form

$$\mathbf{F}(t) = \mathbf{I} + \mathcal{H}(t) (\mathbf{F}_0 - \mathbf{I}) \tag{34}$$

with $\mathcal{H}(t)$ denoting the Heaviside function

$$\mathcal{H}(t) = \begin{cases} 0 & \text{if } t \leq 0 \\ 1 & \text{if } t > 0. \end{cases} \tag{35}$$

Clearly, this loading prescription corresponds to a macroscopic deformation gradient \mathbf{F}_0 that is applied infinitely fast at $t = 0+$.

We are interested in solving (12)–(13) with (34) at time $t = 0+$. To that end, we look for solutions of the form

$$\begin{aligned} \mathbf{y}(\mathbf{X}, t) &= \mathbf{X} + \mathbf{u}_0(\mathbf{X}, t)\mathcal{H}(t), \\ p(\mathbf{X}, t) &= \mu_m + \nu_m + p_0(\mathbf{X}, t)\mathcal{H}(t), \\ \mathbf{C}^v(\mathbf{X}, t) &= \mathbf{I} + t \mathbf{C}_1^v(\mathbf{X}) + O(t^2) \end{aligned} \tag{36}$$

and introduce the notation

$$\mathbf{y}_0(\mathbf{X}) = \mathbf{y}(\mathbf{X}, 0+) = \mathbf{X} + \mathbf{u}_0(\mathbf{X}, 0+).$$

On substitution of (36)₃, noting that

$$\dot{\mathbf{C}}^v = \mathbf{C}_1^v + O(t) \quad \text{and} \quad \mathbf{C}^{v-1} = \mathbf{I} - t \mathbf{C}_1^v + O(t^2),$$

it is a simple matter to solve equation (13) for the internal variable $\mathbf{C}^v(\mathbf{X}, t)$ to leading order to determine that

$$\mathbf{C}_1^v = \frac{\nu_m}{\eta_m} \left[\nabla \mathbf{y}_0^T \nabla \mathbf{y}_0 - \frac{1}{3} (\nabla \mathbf{y}_0 \cdot \nabla \mathbf{y}_0) \mathbf{I} \right].$$

Furthermore, making use of the ansatz (36), it follows that at $t = 0+$ equations (12) simplify to the boundary-value problem

$$\begin{cases} \text{Div} \left[(1 - \theta_b(\mathbf{X})) ((\mu_m + \nu_m) \nabla \mathbf{y}_0 - (\mu_m + \nu_m + p_0) \nabla \mathbf{y}_0^{-T}) \right] = \mathbf{0}, & \mathbf{X} \in \Omega_0 \\ \det \nabla \mathbf{y}_0 = 1, & \mathbf{X} \in \Omega_0^{(m)} \\ \mathbf{y}_0(\mathbf{X}) = \mathbf{F}_0 \mathbf{X}, & \mathbf{X} \in \partial \Omega_0 \end{cases} \tag{37}$$

for the deformation field $\mathbf{y}_0(\mathbf{X})$ and pressure field $p_0(\mathbf{X}, 0+)$.

Once again, equations (37) are the governing equations for the homogenized elastic response of a random isotropic suspension of vacuous bubbles, with characteristic function θ_b , embedded this time in a Gaussian rubber matrix with initial shear modulus $\mu_m + \nu_m$. In line with (33) hence, the macroscopic stress (10) corresponding to a macroscopic deformation gradient \mathbf{F}_0 that is applied infinitely fast at $t = 0+$ is approximately given by the relation

$$\begin{aligned} \mathbf{S}(t) &= \frac{3(1 - f_0)}{3 + 2f_0} (\mu_m + \nu_m) \mathbf{F}_0 + \\ &\quad \frac{\mu_m + \nu_m}{2} \left[\frac{3 + 6J_0 + 2f_0(1 + 7J_0)}{(3 + 2f_0)J_0^{1/3}} + \frac{f_0^{1/3} J_0(4 - 5f_0 - 4J_0)}{(J_0 + f_0 - 1)^{4/3}} \right] \mathbf{F}_0^{-T} + O(t), \end{aligned} \tag{38}$$

where, as above, $J_0 = \det \mathbf{F}_0$.

5 The Homogenized Response at Finite Deformations in the Absence of Storage of Elastic Energy

We now turn to the limiting regime when the rubber matrix loses its ability to store elastic energy and reduces to a Newtonian fluid. As anticipated in Remark 1 above, such a regime corresponds to the choice of material constants $\mu_m = 0$ and $\nu_m \rightarrow +\infty$. The resulting non-linear viscoelasticity problem (12)–(13) specializes then to that of the homogenization of the Stokes flow of an initially random isotropic *suspension of vacuous bubbles in an incompressible Newtonian fluid*.

We begin by setting $\mu_m = 0$ and considering solutions to (12)–(13) of the asymptotic form

$$\begin{aligned} \mathbf{y}(\mathbf{X}, t) &= \mathbf{y}_0(\mathbf{X}, t) + \nu_m^{-1} \mathbf{y}_1(\mathbf{X}, t) + O(\nu_m^{-2}), \\ p(\mathbf{X}, t) &= \nu_m + p_0(\mathbf{X}, t) + O(\nu_m^{-1}), \\ \mathbf{C}^v(\mathbf{X}, t) &= \mathbf{C}_0^v(\mathbf{X}, t) + \nu_m^{-1} \mathbf{C}_1^v(\mathbf{X}, t) + O(\nu_m^{-2}) \end{aligned} \tag{39}$$

in the limit as $\nu_m \rightarrow +\infty$. On substitution of (39)₃, noting that

$$\dot{\mathbf{C}}^v = \dot{\mathbf{C}}_0^v + \nu_m^{-1} \dot{\mathbf{C}}_1^v + O(\nu_m^{-2}) \quad \text{and} \quad \mathbf{C}^{v-1} = \mathbf{C}_0^{v-1} - \nu_m^{-1} \mathbf{C}_0^{v-1} \mathbf{C}_1^v \mathbf{C}_0^{v-1} + O(\nu_m^{-2}),$$

standard calculations show that $O(\nu_m)$ and $O(\nu_m^0)$ of the expansion of equation (13) yield the solutions

$$\mathbf{C}_0^v = \nabla \mathbf{y}_0^T \nabla \mathbf{y}_0 \tag{40}$$

and

$$\begin{aligned} \mathbf{C}_1^v &= -\eta_m \dot{\mathbf{C}}_0^v + \frac{1}{3} (\mathbf{C}_1^v \cdot \mathbf{C}_0^{v-1}) \mathbf{C}_0^v + \nabla \mathbf{y}_0^T \nabla \mathbf{y}_1 + \nabla \mathbf{y}_1^T \nabla \mathbf{y}_0 - \\ &\frac{1}{3} [(\nabla \mathbf{y}_0^T \nabla \mathbf{y}_1 + \nabla \mathbf{y}_1^T \nabla \mathbf{y}_0) \cdot \mathbf{C}_0^{v-1}] \mathbf{C}_0^v. \end{aligned} \tag{41}$$

Now, making direct use of the ansatz (39) together with the results (40), (41), and a change of Lagrangian to Eulerian variables, the equation of leading $O(\nu_m^0)$ emerging from (12) reduces to the initial-boundary-value problem

$$\begin{cases} \operatorname{div} [(1 - \chi_b(\mathbf{x})) (\eta_m (\nabla_{\mathbf{x}} \mathbf{v} + \nabla_{\mathbf{x}} \mathbf{v}^T) - q \mathbf{I})] = \mathbf{0}, & (\mathbf{x}, t) \in \Omega(t) \times [0, T] \\ \operatorname{tr} \nabla \mathbf{v} = 0, & (\mathbf{x}, t) \in \Omega^{(m)}(t) \times [0, T] \\ \mathbf{v}(\mathbf{x}, t) = \dot{\mathbf{F}}(t) \mathbf{F}^{-1}(t) \mathbf{x}, & (\mathbf{x}, t) \in \partial \Omega(t) \times [0, T] \end{cases} \tag{42}$$

for the velocity $\mathbf{v}(\mathbf{y}_0(\mathbf{X}, t), t) = \dot{\mathbf{y}}_0(\mathbf{X}, t)$ and pressure $q(\mathbf{x}, t)$ fields, where use has been made of the notation $\chi_b(\mathbf{y}_0(\mathbf{X}, t)) = \theta_b(\mathbf{X})$ and $\nabla_{\mathbf{x}} \mathbf{v}(\mathbf{x}, t) = \partial \mathbf{v}(\mathbf{x}, t) / \partial \mathbf{x}$.

Equations (42) are the governing equations for the homogenized *viscous* response of a suspension of vacuous bubbles, with characteristic function χ_b , in an incompressible Newtonian fluid with viscosity η_m under conditions of Stokes flow in the absence of surface tension between the bubbles and the fluid. At any given *fixed* time $t \in [0, T]$, the problem (42) is thus mathematically equivalent to the *linear* elastostatics problem (19) that arises in the limit of small deformations. It then follows that the volume average

$$\mathbf{T}(t) := \frac{1}{|\Omega(t)|} \int_{\Omega(t)} \mathbf{T}(\mathbf{x}, t) d\mathbf{x}$$

of the pointwise Cauchy stress

$$\mathbf{T}(\mathbf{x}, t) = (1 - \chi_b(\mathbf{x})) (\eta_m (\nabla_{\mathbf{x}} \mathbf{v} + \nabla_{\mathbf{x}} \mathbf{v}^T) - q \mathbf{I})$$

over the current configuration $\Omega(t)$ is simply given by the effective relation

$$\mathbf{T}(t) = \overline{\mathcal{M}} \mathbf{D}, \tag{43}$$

where $\mathbf{D}(t) = \frac{1}{2}(\dot{\mathbf{F}}\mathbf{F}^{-1} + \mathbf{F}^{-T}\dot{\mathbf{F}}^T)$ denotes the macroscopic rate of deformation tensor and $\overline{\mathcal{M}}$ stands for the effective viscosity tensor

$$\overline{\mathcal{M}}_{ijkl} = \frac{\eta_m}{|\Omega(t)|} \int_{\Omega(t)} (1 - \chi_b(\mathbf{x})) \left(2\mathcal{K}_{ijmn} \frac{\partial \gamma_{mkl}}{\partial x_n}(\mathbf{x}) - \delta_{ij} \sigma_{kl}(\mathbf{x}) \right) d\mathbf{x}. \tag{44}$$

In this last expression, in entire analogy with (21), $\boldsymbol{\gamma}(\mathbf{x})$ and $\boldsymbol{\sigma}(\mathbf{x})$ are the concentration tensors solution of the linear “elastostatics” problem

$$\begin{cases} \frac{\partial}{\partial x_j} \left[(1 - \chi_b(\mathbf{x})) \left(\mathcal{K}_{ijmn} \frac{\partial \gamma_{mkl}}{\partial x_n}(\mathbf{x}) - \frac{1}{2} \delta_{ij} \sigma_{kl}(\mathbf{x}) \right) \right] = 0, & \mathbf{x} \in \Omega(t) \\ \frac{\partial \gamma_{mkl}}{\partial x_m}(\mathbf{x}) = 0, & \mathbf{x} \in \Omega^{(m)}(t) \\ \gamma_{ikl}(\mathbf{x}) = \delta_{ik} x_l, & \mathbf{x} \in \partial\Omega(t). \end{cases}$$

In view of the result (43), by virtue of the connection $\mathbf{S}(t) = |\Omega_0|^{-1} \int_{\Omega_0} \mathbf{S}(\mathbf{X}, t) d\mathbf{X} = |\Omega(t)|^{-1} \int_{\Omega(t)} \mathbf{T}(\mathbf{x}, t) \nabla_{\mathbf{x}} \mathbf{X}^T d\mathbf{x} = \mathbf{J} \mathbf{T}(t) \mathbf{F}^{-T}$ between the macroscopic first Piola-Kirchhoff and Cauchy stress tensors, it is a simple matter to conclude that the macroscopic stress (10) is given asymptotically by

$$\mathbf{S}(t) = \frac{J}{2} \overline{\mathcal{M}} \left(\dot{\mathbf{F}}\mathbf{F}^{-1} \mathbf{F}^{-T} + \mathbf{F}^{-T} \dot{\mathbf{F}}^T \mathbf{F}^{-T} \right) + O(v_m^{-1}) \tag{45}$$

in the limit as $\mu_m = 0$ and $v_m \rightarrow +\infty$, where $J = \det \mathbf{F}$.

Remark 4 The first study of the problem (42) can be traced back to the work of Taylor [24] in the 1930s. Since then, as outlined in several review articles throughout the past four decades [25–27], significant progress has been made on all relevant theoretical, computational, and experimental aspects; nevertheless, most studies have focused on particular types of isochoric flows and not on flows involving changes in volume. At present, it is thus well established that the response (45), or equivalently (43), is in general *non-Newtonian*. This is because the effective viscosity tensor (44) is not a constant but rather a function of the deformation history via the evolution in time of the characteristic function χ_b , which encodes how all the bubbles in the suspension deform in space along the given loading path.

Irrespectively of how χ_b evolves in time, however, thanks to the variational character of the governing equations, the effective viscosity tensor (44) can be bounded from above [28]. Precisely, regardless of the loading conditions, the effective viscosity tensor (44) is bounded from above according to the Voigt bound

$$\overline{\mathcal{M}} \leq \overline{\mathcal{M}}^V = 2\overline{\eta}_{\mathcal{K}}^V \mathcal{K} + 3\overline{\eta}_{\mathcal{J}}^V \mathcal{J} \quad \text{with} \quad \overline{\eta}_{\mathcal{K}}^V = (1 - f)\eta_m \quad \text{and} \quad \overline{\eta}_{\mathcal{J}}^V = +\infty. \tag{46}$$

Furthermore, for loading conditions for which the suspension remains isotropic, (44) is bounded from above according to the tighter HS bound

$$\begin{aligned} \overline{\mathcal{M}} &\leq \overline{\mathcal{M}}^{HS} = 2\overline{\eta}_{\mathcal{K}}^{HS} \mathcal{K} + 3\overline{\eta}_{\mathcal{J}}^{HS} \mathcal{J} \quad \text{with} \\ \overline{\eta}_{\mathcal{K}}^{HS} &= \frac{3(1-f)}{3+2f} \eta_m \quad \text{and} \quad \overline{\eta}_{\mathcal{J}}^{HS} = \frac{4(1-f)}{3f} \eta_m. \end{aligned} \tag{47}$$

In these last expressions, the inequalities are meant in the sense of quadratic forms and

$$f := \frac{1}{|\Omega(t)|} \int_{\Omega(t)} \chi_b(\mathbf{x}) \, d\mathbf{x} = \frac{J-1}{J} + \frac{f_0}{J} \tag{48}$$

denotes the volume fraction of bubbles in the current configuration $\Omega(t)$. Clearly, in view of (48), both variational approximations (46) and (47) describe non-Newtonian viscosities.

6 Sample Computational Results for Suspensions of Initially Monodisperse Spherical Bubbles

As already stressed above, for general macroscopic deformation gradients $\mathbf{F}(t)$ and general material constants μ_m, ν_m, η_m , the governing equations (12)–(13) defining the macroscopic response (10)–(11) of the suspension can only be solved numerically. In this section, we make use of the scheme introduced in [1] to generate solutions for the macroscopic response of an elementary type of suspension, that of initially spherical bubbles of monodisperse size. Notably, the scheme makes use of a conforming Crouzeix-Raviart FE discretization of space and a high-order accurate explicit Runge-Kutta discretization of time. The combination of these two types of discretizations results into a stable scheme that is capable of handling finite deformations and the incompressibility constraint of the rubber for general loading conditions, irrespectively of whether they are applied slowly, fast, or span a large time range.

Following a well-settled approach [16, 29–33], we idealize the suspension as a periodic medium where the periodically repeated unit cell contains a random isotropic distribution

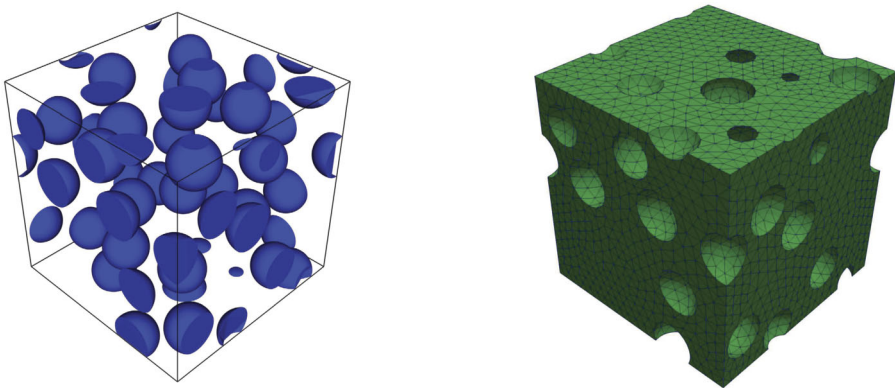


Fig. 3 Representative unit cell containing $N_b = 30$ randomly distributed initially spherical bubbles of monodisperse size at volume fraction $f_0 = 0.15$ and its FE discretization with approximately 100,000 elements

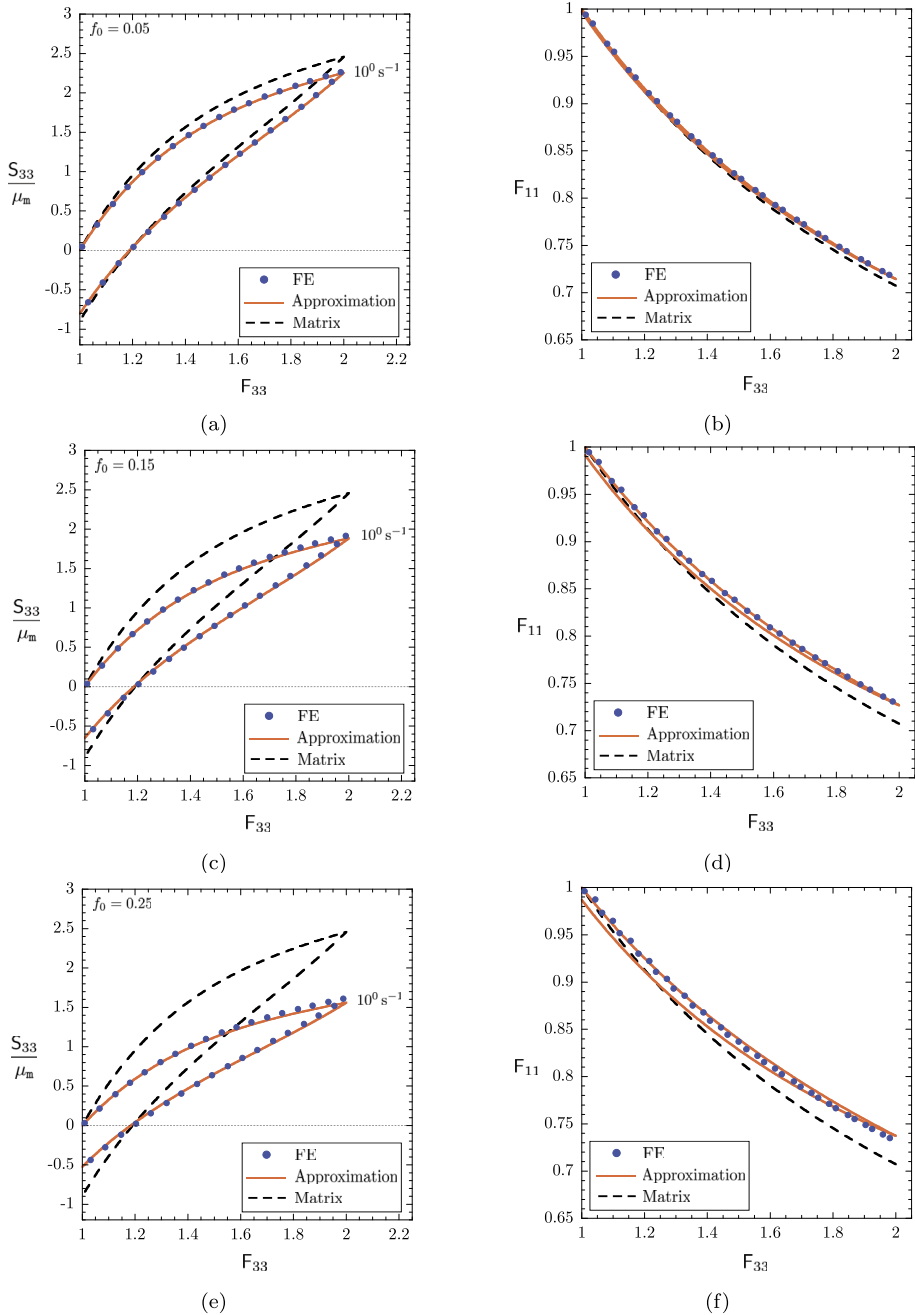


Fig. 4 Macroscopic response of suspensions of monodisperse spherical bubbles in a rubber matrix with material constants $\nu_m = \mu_m$, $\tau_m = \eta_m/\nu_m = 1$ s for a uniaxial tension loading/unloading cycle at constant stretch rate $|\dot{F}_{33}| = 10^0 \text{ s}^{-1}$. The results show the normalized stress S_{33}/μ_m and the lateral stretch F_{11} as functions of the applied stretch F_{33} for suspensions with initial volume fractions of bubbles: (a)–(b) $f_0 = 0.05$, (c)–(d) $f_0 = 0.15$, and (e)–(f) $f_0 = 0.25$. This and all subsequent figures include, for direct comparison, the predictions generated by the proposed approximation (56)–(57)

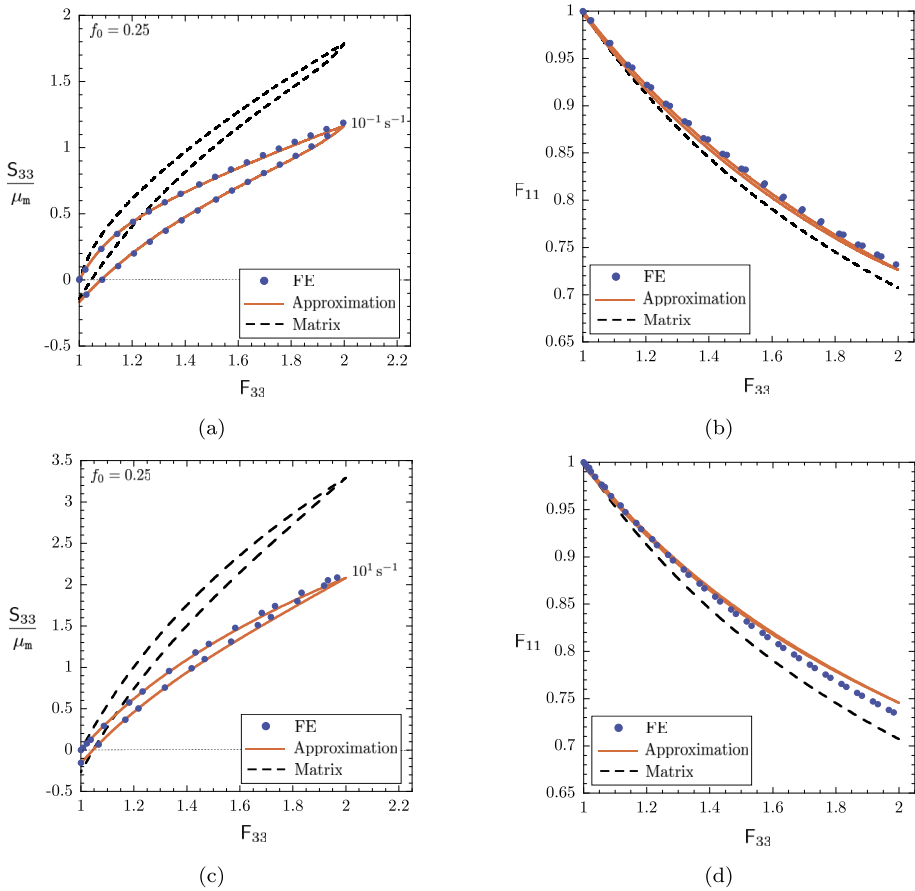


Fig. 5 Macroscopic response of a suspension of monodisperse spherical bubbles, with initial volume fraction $f_0 = 0.25$, in a rubber matrix, with material constants $\nu_m = \mu_m$, $\tau_m = \eta_m/\nu_m = 1$ s, for uniaxial tension loading/unloading cycles at two different constant stretch rates. The results show the normalized stress S_{33}/μ_m and the lateral stretch F_{11} as functions of the applied stretch F_{33} for constant stretch rates: (a)–(b) $|\dot{F}_{33}| = 10^{-1} \text{ s}^{-1}$ and (c)–(d) $|\dot{F}_{33}| = 10^1 \text{ s}^{-1}$

of a sufficiently large but finite number N_b of vacuous bubbles that approximates the actual random isotropic suspension. For the problem of interest here, that number is $N_b = 30$. Figure 3 shows a representative unit cell at volume fraction $f_0 = 0.15$ alongside its FE discretization with approximately 100,000 elements; save for a few exceptions, meshes of this size were checked to yield converged solutions for all the cases that we examined. We do not dwell any further on the computational details and refer the interested reader to Sects. 6 and 7 in [1] for those.

Before proceeding with the presentation of the results *per se*, a few comments are in order. The selection of results included here correspond to a fairly broad spectrum of loading conditions — uniaxial tension, equibiaxial tension, and hydrostatic tension — that involve both macroscopic deformations that are nearly isochoric as well as macroscopic deformations where there are significant changes in volume. The time-dependence of the selected applied loading conditions is such that the nonlinear viscous dissipation of the underlying

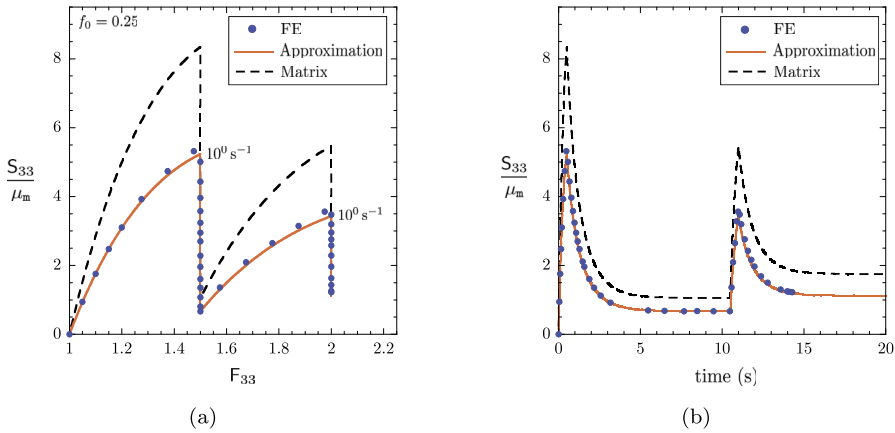


Fig. 6 Macroscopic response of a suspension of monodisperse spherical bubbles, with initial volume fraction $f_0 = 0.25$, in a rubber matrix, with material constants $\nu_m = 10\mu_m$ and $\tau_m = \eta_m/\nu_m = 1 \text{ s}$, for a two-step relaxation test in uniaxial tension where the stretch is increased at the same constant rate $\dot{F}_{33} = 10^0 \text{ s}^{-1}$ for the two loading steps. (a) The normalized stress-stretch relation. (b) The normalized stress-time relation

rubber matrix is fully probed between the asymptotic limits of slow and fast rates discussed in Sects. 4.1 and 4.2. Moreover, the deformation range of the selected applied loadings conditions is such that the nonlinear (equilibrium and non-equilibrium) elasticity of the rubber is also fully probed.

Uniaxial Tension Figures 4 through 6 present results for various types of uniaxial tension loading conditions with $\mathbf{F}(t) = F_{11}(t)(\mathbf{e}_1 \otimes \mathbf{e}_1 + \mathbf{e}_2 \otimes \mathbf{e}_2) + F_{33}(t)\mathbf{e}_3 \otimes \mathbf{e}_3$ and $\mathbf{S}(t) = S_{33}(t)\mathbf{e}_3 \otimes \mathbf{e}_3$, where again $\{\mathbf{e}_i\}$ $i = 1, 2, 3$ stands for the laboratory frame of reference and $F_{33}(t) \geq 1$ is prescribed.

Specifically, Fig. 4 presents results for the stress S_{33}/μ_m , normalized by the initial equilibrium shear modulus μ_m of the underlying rubber matrix, and for the lateral stretch F_{11} as functions of the applied stretch F_{33} for the case when F_{33} is first increased to $F_{33} = 2$ and subsequently decreased back to $F_{33} = 1$ at the same constant stretch rate of $|\dot{F}_{33}| = 10^0 \text{ s}^{-1}$ for both the loading and the unloading branches. The results in Figs. 3(a)–(b) pertain to a suspension with $f_0 = 0.05$ volume fraction of bubbles, while those in Figs. 3(c)–(d) and (e)–(f) correspond to suspensions with $f_0 = 0.15$ and 0.25 , respectively. Figure 5 presents similar results for S_{33}/μ_m and F_{11} as functions of F_{33} for a suspension with volume fraction of bubbles $f_0 = 0.25$ at two different constant stretch rates, $|\dot{F}_{33}| = 10^{-1}$ and 10^1 s^{-1} . All the results in Figs. 4 and 5 pertain to suspensions wherein the rubber matrix has initial non-equilibrium shear modulus $\nu_m = \mu_m$, initial relaxation time³ $\tau_m = 1 \text{ s}$, and hence viscosity $\eta_m = \tau_m \nu_m = \mu_m \text{ s}$.

Figure 6 presents results for a two-step relaxation test, wherein F_{33} is first increased to $F_{33} = 1.50$ at the constant stretch rate of $|\dot{F}_{33}| = 10^0 \text{ s}^{-1}$, then held fixed for a time of $t = 10 \text{ s}$, then increased to $F_{33} = 2$ at the same constant stretch rate of $|\dot{F}_{33}| = 10^0 \text{ s}^{-1}$, and then held fixed again for the same amount of time $t = 10 \text{ s}$. The results pertain to a suspension with $f_0 = 0.25$ volume fraction of bubbles wherein the rubber matrix has initial

³Here and subsequently, for notational simplicity and without loss in generality, we use s as the unit of time. The choice of relaxation time $\tau_m = 1 \text{ s}$ implies then that the time scale is normalized by the relaxation time τ_m of the rubber matrix, whatever this may be.

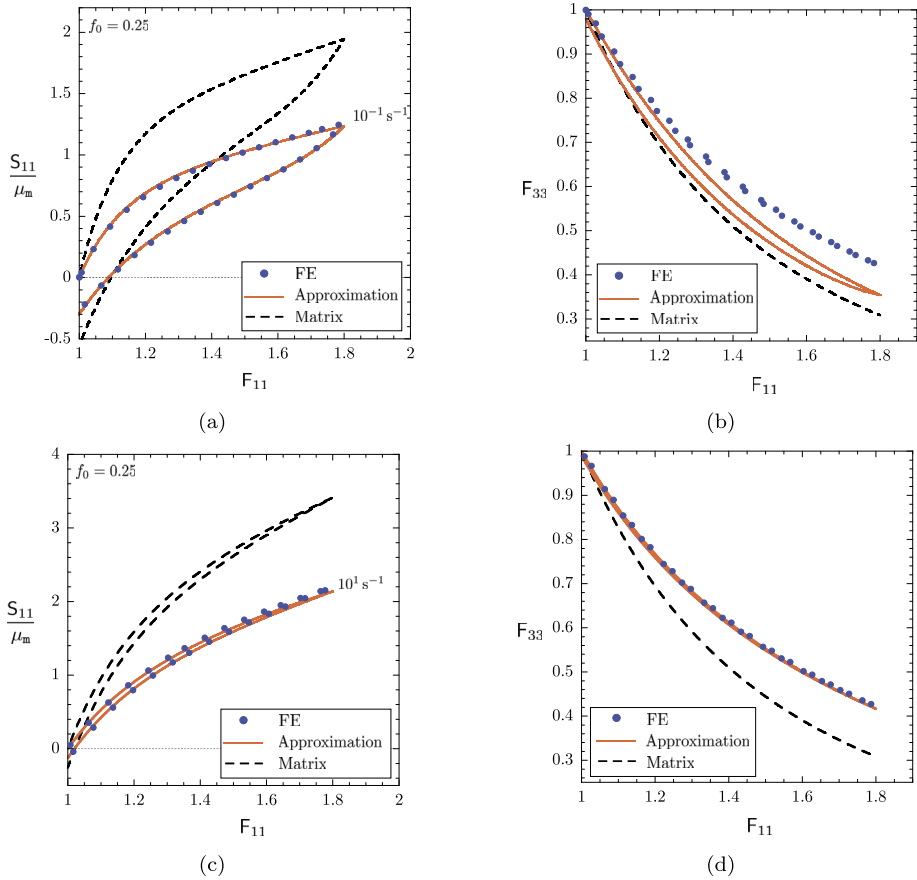


Fig. 7 Macroscopic response of a suspension of monodisperse spherical bubbles, with initial volume fraction $f_0 = 0.25$, in a rubber matrix, with material constants $\nu_m = \mu_m$, $\tau_m = \eta_m/\nu_m = 1$ s, for equibiaxial tension loading/unloading cycles at two different constant stretch rates. The results show the normalized stress S_{11}/μ_m and the lateral stretch F_{33} as functions of the applied stretch F_{11} for constant stretch rates: (a)–(b) $|\dot{F}_{11}| = 10^{-1} \text{ s}^{-1}$ and (c)–(d) $|\dot{F}_{11}| = 10^1 \text{ s}^{-1}$

non-equilibrium shear modulus $\nu_m = 10\mu_m$, initial relaxation time $\tau_m = 1$ s, and hence viscosity $\eta_m = \tau_m\nu_m = 10\mu_m$ s. While Fig. 6(a) shows the stress-stretch relation, Fig. 6(b) shows the corresponding stress-time relation.

Equibiaxial Tension Figures 7 and 8 present results entirely analogous to those of Figs. 5 and 6 for loading conditions of equibiaxial tension with $\mathbf{F}(t) = F_{11}(t)(\mathbf{e}_1 \otimes \mathbf{e}_1 + \mathbf{e}_2 \otimes \mathbf{e}_2) + F_{33}(t)\mathbf{e}_3 \otimes \mathbf{e}_3$ and $\mathbf{S}(t) = S_{11}(t)(\mathbf{e}_1 \otimes \mathbf{e}_1 + \mathbf{e}_2 \otimes \mathbf{e}_2)$, where $F_{11}(t) \geq 1$ is prescribed.

Hydrostatic Tension Finally, Figs. 9 and 10 present results analogous to those of Figs. 5 and 6 for loading conditions of hydrostatic tension with $\mathbf{F}(t) = \lambda(t)\mathbf{I}$ and $\mathbf{S}(t) = S(t)\mathbf{I}$, where $\lambda(t) \geq 1$ is prescribed.

For direct comparison with the computational results for the suspensions (solid circles), whenever possible (recall that the rubber matrix is incompressible), the plots in Figs. 4 through 10 include the corresponding results for the rubber matrix without bubbles (dashed

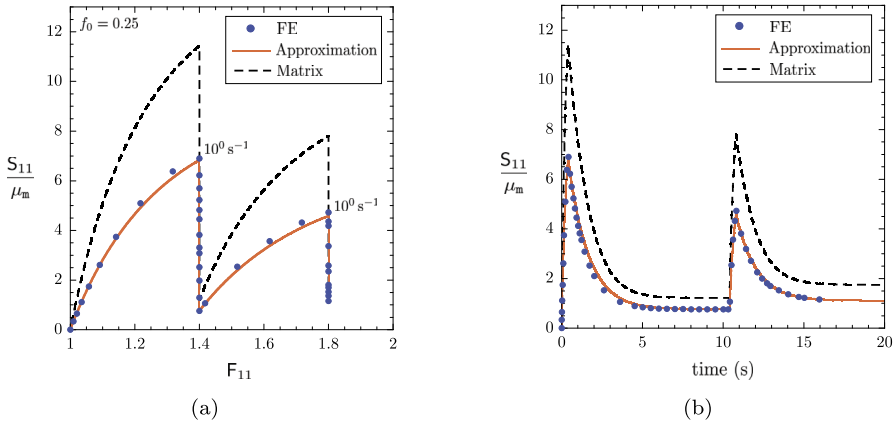


Fig. 8 Macroscopic response of a suspension of monodisperse spherical bubbles, with initial volume fraction $f_0 = 0.25$, in a rubber matrix, with material constants $\nu_m = 10\mu_m$ and $\tau_m = \eta_m/\nu_m = 1$ s, for a two-step relaxation test in equibiaxial tension where the stretch is increased at the same constant rate $\dot{F}_{11} = 10^0 \text{ s}^{-1}$ for the two loading steps. **(a)** The normalized stress-stretch relation. **(b)** The normalized stress-time relation

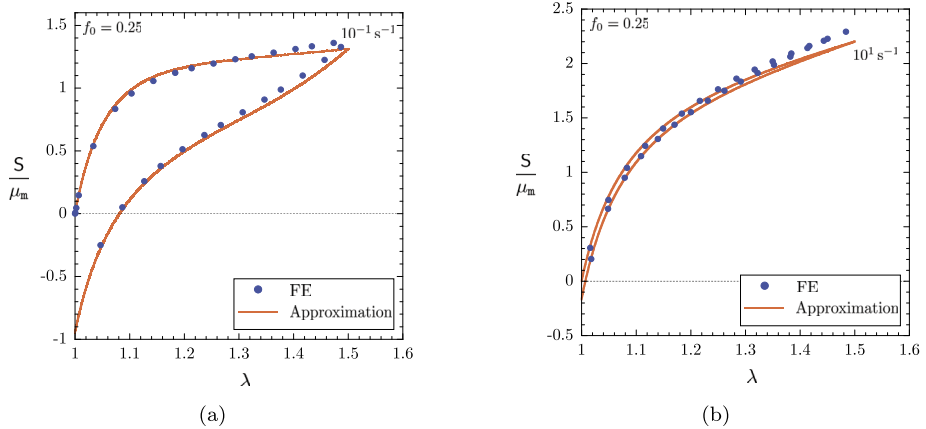


Fig. 9 Macroscopic response of a suspension of monodisperse spherical bubbles, with initial volume fraction $f_0 = 0.25$, in a rubber matrix, with material constants $\nu_m = \mu_m$, $\tau_m = \eta_m/\nu_m = 1$ s, for hydrostatic tension loading/unloading cycles at two different constant stretch rates. The results show the normalized stress S/μ_m as a function of the applied stretch λ for constant stretch rates: **(a)** $|\dot{\lambda}| = 10^{-1} \text{ s}^{-1}$ and **(b)** $|\dot{\lambda}| = 10^1 \text{ s}^{-1}$

lines). All the plots include as well the results based on the approximate solution (solid lines) introduced in the next section.

The central observation from all of the above computational results is that the behavior of the suspension is qualitatively similar to the short-range-memory behavior of the underlying rubber matrix. What is more, the results suggest that the effective viscosity of the suspension is not constant, like that of the underlying rubber matrix, but rather a function of the deformation history. The agreement shown by all the figures between the computational results and the approximate solution described next provide quantitative evidence that this may indeed be the case.

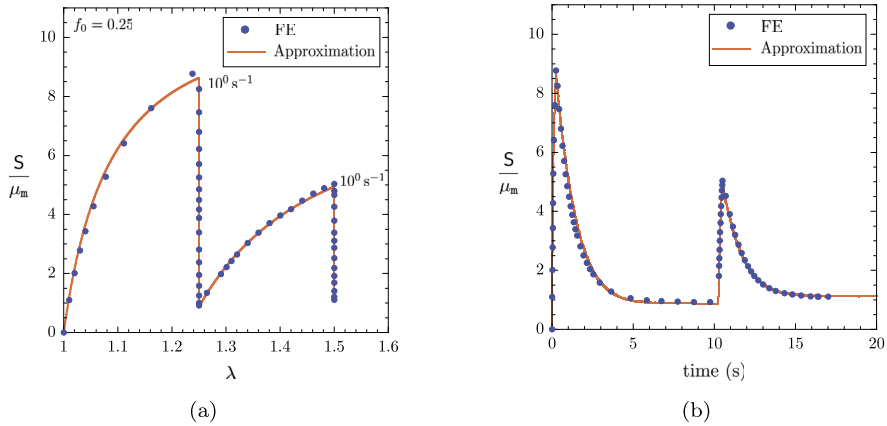


Fig. 10 Macroscopic response of a suspension of monodisperse spherical bubbles, with initial volume fraction $f_0 = 0.25$, in a rubber matrix, with material constants $\nu_m = 10\mu_m$ and $\tau_m = \eta_m/\nu_m = 1$ s, for a two-step relaxation test in hydrostatic tension where the stretch is increased at the same constant rate $\dot{\lambda} = 10^0 \text{ s}^{-1}$ for the two loading steps. (a) The normalized stress-stretch relation. (b) The normalized stress-time relation

7 An Approximate Solution

The asymptotic results presented in Sects. 3 through 5 together with the computational results presented in Sect. 6 suggest that the constitutive relation (10)–(11) that describes the macroscopic viscoelastic response of the suspensions of interest in this work is of the same functional form as that describing the underlying rubber matrix, *with the distinctive differences that their effective elasticity is compressible and their effective viscosity is compressible and nonlinear*. Precisely, the results suggest that the macroscopic constitutive relation (10)–(11) can be cast within the two-potential framework as

$$\mathbf{S}(t) = \frac{\partial \Psi}{\partial \mathbf{F}}(\mathbf{F}, \mathbf{F}^v) \quad \text{with evolution equation} \quad \begin{cases} \frac{\partial \Psi}{\partial \mathbf{F}^v}(\mathbf{F}, \mathbf{F}^v) + \frac{\partial \Phi}{\partial \mathbf{F}^v}(\mathbf{F}, \mathbf{F}^v, \dot{\mathbf{F}}^v) = \mathbf{0} \\ \mathbf{F}^v(0) = \mathbf{I} \end{cases} \quad (49)$$

in terms of an effective free energy of the form

$$\Psi(\mathbf{F}, \mathbf{F}^v) = \Psi^{\text{Eq}}(\mathbf{F}) + J^v \Psi^{\text{NEq}}(\mathbf{F}\mathbf{F}^{v-1}, \mathbf{F}^v) \quad (50)$$

and an effective dissipation potential of the form

$$\Phi(\mathbf{F}, \mathbf{F}^v, \dot{\mathbf{F}}^v) = \frac{1}{2} \dot{\mathbf{F}}^v \mathbf{F}^{v-1} \cdot [J^v \mathbf{M}(\mathbf{F}, \mathbf{F}^v) \dot{\mathbf{F}}^v \mathbf{F}^{v-1}] \quad \text{with } \mathbf{M} = 2m_{\mathcal{K}}(\mathbf{F}, \mathbf{F}^v)\mathcal{K} + 3m_{\mathcal{J}}(\mathbf{F}, \mathbf{F}^v)\mathcal{J}, \quad (51)$$

where \mathbf{F}^v is the macroscopic internal variable of state that describes roughly the “viscous part” of the macroscopic deformation gradient \mathbf{F} ,

$$J^v = \det \mathbf{F}^v,$$

Ψ^{Eq} and Ψ^{NEq} are the effective stored-energy functions that characterize, respectively, the elastic energy storage in the given suspension at states of thermodynamic equilibrium

and the additional elastic energy storage at non-equilibrium states, while $m_{\mathcal{K}}(\mathbf{F}, \mathbf{F}^v)$ and $m_{\mathcal{J}}(\mathbf{F}, \mathbf{F}^v)$ characterize its effective nonlinear deviatoric and volumetric viscosity.

7.1 Approximation of the Effective Free-Energy Functions Ψ^{Eq} and Ψ^{NEq}

In particular, the results in Sects. 3 and 4 suggest that Ψ^{Eq} and Ψ^{NEq} correspond to the free-energy functions that describe the homogenized *elastic* responses of two different suspensions of vacuous bubbles in two different Gaussian rubber matrices. More specifically, they suggest that the former corresponds to the given suspension, with initial characteristic function θ_b , in a Gaussian rubber matrix with initial shear modulus μ_m , while the latter corresponds to a suspension with a different characteristic function χ_b^v , the one that results from subjecting the initial suspension to a macroscopic deformation gradient \mathbf{F}^v , in a different Gaussian rubber matrix with initial shear modulus ν_m . As already noted at the end of Sect. 4.1, accurate explicit approximations for these effective free-energy functions have been recently introduced in [16]. They read

$$\Psi^{\text{Eq}}(\mathbf{F}) = \frac{3(1 - f_0)}{2(3 + 2f_0)} \mu_m [I_1 - 3] + \frac{3\mu_m}{2J^{1/3}} \left[2J - 1 - \frac{(1 - f_0)J^{1/3} (3J^{2/3} + 2f_0)}{3 + 2f_0} - \frac{f_0^{1/3}J^{1/3} (2J + f_0 - 2)}{(J - 1 + f_0)^{1/3}} \right] \tag{52}$$

and

$$\Psi^{\text{NEq}}(\mathbf{F}\mathbf{F}^{v-1}, \mathbf{F}^v) = \frac{3(1 - f^v)}{2(3 + 2f^v)} \nu_m [I_1^e - 3] + \frac{3\nu_m}{2J^e{}^{1/3}} \left[2J^e - 1 - \frac{(1 - f^v)J^e{}^{1/3} (3J^e{}^{2/3} + 2f^v)}{3 + 2f^v} - \frac{f^v{}^{1/3}J^e{}^{1/3} (2J^e + f^v - 2)}{(J^e - 1 + f^v)^{1/3}} \right], \tag{53}$$

where

$$I_1 = \mathbf{F} \cdot \mathbf{F} = \text{tr } \mathbf{C}, \quad J = \det \mathbf{F} = \sqrt{\det \mathbf{C}},$$

$$I_1^e = \mathbf{F}\mathbf{F}^{v-1} \cdot \mathbf{F}\mathbf{F}^{v-1} = \text{tr}(\mathbf{C}\mathbf{C}^{v-1}), \quad J^e = \det(\mathbf{F}\mathbf{F}^{v-1}) = \frac{J}{J^v} = \frac{\sqrt{\det \mathbf{C}}}{\sqrt{\det \mathbf{C}^v}},$$

and

$$f^v = \frac{J^v - 1}{J^v} + \frac{f_0}{J^v}$$

with $\mathbf{C} = \mathbf{F}^T \mathbf{F}$ and $\mathbf{C}^v = \mathbf{F}^{vT} \mathbf{F}^v$.

7.2 Approximation of the Effective Viscosities $m_{\mathcal{K}}$ and $m_{\mathcal{J}}$

Moreover, initially at time $t = 0$, when $\mathbf{F}(0) = \mathbf{F}^v(0) = \mathbf{I}$ and the microstructure of the given suspension is described by the characteristic function θ_b , the asymptotic result in Sect. 3 indicates that the effective viscosities take the values $m_{\mathcal{K}}(\mathbf{I}, \mathbf{I}) = \bar{\eta}_{\mathcal{K}}$ and $m_{\mathcal{J}}(\mathbf{I}, \mathbf{I}) = \bar{\eta}_{\mathcal{J}}$, where we recall that the effective material constants $\bar{\eta}_{\mathcal{K}}$ and $\bar{\eta}_{\mathcal{J}}$ are given by expressions (29). As the suspension is finitely deformed and the characteristic function of the bubbles

evolves to χ_b , the asymptotic result in Sect. 5 indicates furthermore that the viscosities m_K and $m_{\mathcal{J}}$ may not remain constant at (29) but that, instead, may be functions of the deformation history.

Direct comparisons with a wide spectrum of computational results, a representative sample of which have been presented in Sect. 6 above, reveal that the HS variational result (47)₂ evaluated at a volume fraction of bubbles f^v , corresponding to the microstructure that results from deforming the initial suspension by the “viscous part” \mathbf{F}^v of the macroscopic deformation gradient \mathbf{F} , provides a simple yet fairly accurate approximation for the effective deviatoric viscosity m_K . With some abuse of notation, we thus set

$$m_K(\mathbf{F}, \mathbf{F}^v) = m_K(J^v) = \frac{3(1 - f^v)}{3 + 2f^v} \eta_m = \frac{3(1 - f_0)}{5J^v - 2(1 - f_0)} \eta_m. \tag{54}$$

On the other hand, the analysis presented separately in the Appendix to avoid loss of continuity, has revealed that, again with some abuse of notation, the formula

$$m_{\mathcal{J}}(\mathbf{F}, \mathbf{F}^v) = m_{\mathcal{J}}(J, J^v) = \frac{20J^{4/3} (J + f_0 - 1)^{4/3}}{\Xi(J, J^v)} \times \left(\frac{J^v (J - 2J^v - f_0 + 1)}{(J^v + f_0 - 1)^{2/3} (J + f_0 - 1)^{1/3}} + \frac{2J^{v4/3}}{J^{1/3}} - J^{v1/3} J^{2/3} \right) \times \left(\frac{J^{v2/3} J^{4/3} (J^v + J + 2f_0 - 2)}{(J^v + f_0 - 1)^{1/3}} - (J^v + f_0 - 1)^{1/3} (J + f_0 - 1)^{4/3} (J^v + J) \right) \eta_m \tag{55}$$

with

$$\begin{aligned} \Xi(J, J^v) = & J^{v2/3} J^{8/3} [3(1 - f_0)^3 - (1 - f_0)^2 (41J^v - 32J) + \\ & (1 - f_0) (36J^v J + 23J^{v2} - 50J^2) - 8J^{v2} J - 10J^v J^2 - 5J^{v3} + 20J^3] + \\ & J^{v1/3} (J^v + f_0 - 1)^{1/3} (J + f_0 - 1)^{8/3} (8J^{v2} J + 10J^v J^2 + 5J^{v3} - 20J^3) \end{aligned}$$

describes fairly accurately the effective volumetric viscosity $m_{\mathcal{J}}$ of all the suspensions that we have examined. We should emphasize that the choices (54) and (55) are just two plausible approximations for the effective deviatoric and volumetric viscosities of the suspensions that are indeed consistent with all the asymptotic and computational results presented in the preceding sections. More refined approximations are certainly within reach, but we favor (54) and (55) in this first work for their explicit form and theoretical underpinnings.

7.3 The Proposed Approximate Homogenization Solution

Use of the approximations (52)–(55) in the effective free-energy function (50) and the effective dissipation potential (51), and of these in relation (49), leads to the approximation for the macroscopic constitutive relation

$$\begin{aligned} \mathbf{S}(t) = & \frac{3(1 - f_0)}{3 + 2f_0} \mu_m \mathbf{F} + \frac{3(1 - f_0)J^v}{5J^v + 2f_0 - 2} \nu_m \mathbf{F} \mathbf{C}^{v-1} + \\ & \frac{\mu_m}{2} \left[\frac{3 + 6J + 2f_0(1 + 7J)}{(3 + 2f_0)J^{1/3}} + \frac{f_0^{1/3} J(4 - 5f_0 - 4J)}{(J + f_0 - 1)^{4/3}} \right] \mathbf{F}^{-T} + \end{aligned}$$

$$\frac{\nu_m J^v}{2} \left[\frac{J^{2/3}}{J^{v2/3}} \left(7 + \frac{J^v}{J} - \frac{15J^v}{5J^v + 2f_0 - 2} \right) - \frac{J(J^v + f_0 - 1)^{1/3}(J^v + 4J + 5f_0 - 5)}{(J + f_0 - 1)^{4/3}J^v} \right] \mathbf{F}^{-T}, \tag{56}$$

where \mathbf{C}^v is defined by the evolution equation

$$\begin{cases} \dot{\mathbf{C}}^v(t) = \frac{\nu_m}{\eta_m} \mathbf{C} + \frac{2\nu_m}{3\eta_m} \left[\frac{\eta_m}{m_{\mathcal{J}}(J, J^v)} \left(\frac{2J^v - J}{J^{1/3}J^{v2/3}} + \frac{J - 2J^v - f_0 + 1}{(J + f_0 - 1)^{1/3}(J^v + f_0 - 1)^{2/3}} - \frac{3J^{2/3}(1 - f_0)(5J^v - f_0 + 1)}{J^{v2/3}(5J^v + 2f_0 - 2)^2} \right) + \left(\frac{(1 - f_0)(5J^v - f_0 + 1)\eta_m}{(5J^v + 2f_0 - 2)^2 m_{\mathcal{J}}(J, J^v)} - \frac{1}{2} \right) \mathbf{C} \cdot \mathbf{C}^{v-1} \right] \mathbf{C}^v \\ \mathbf{C}^v(0) = \mathbf{I}. \end{cases} \tag{57}$$

Exactly as its local counterpart (8), the dependence on the macroscopic internal variable \mathbf{F}^v enters (56) and (57) only through the symmetric combination $\mathbf{C}^v = \mathbf{F}^{vT} \mathbf{F}^v$. In the sequel, we spell out a number of pertinent remarks.

Remark 5 (The limit of small deformations) In the limit of small deformations as $\|\mathbf{F}(t) - \mathbf{I}\| = \|\mathbf{H}(t)\| \rightarrow 0$, following a calculation akin to that detailed in Sect. 3, it is straightforward to show that the macroscopic response (56)–(57) reduces asymptotically to

$$\mathbf{S}(t) = 2\bar{\mu}^{HS} \left[\boldsymbol{\varepsilon} - \frac{1}{3} \text{tr}(\boldsymbol{\varepsilon}) \mathbf{I} \right] + \bar{\kappa}^{HS} \text{tr}(\boldsymbol{\varepsilon}) \mathbf{I} + 2\bar{\nu}^{HS} \left[\boldsymbol{\varepsilon} - \boldsymbol{\varepsilon}^v - \frac{1}{3} \text{tr}(\boldsymbol{\varepsilon} - \boldsymbol{\varepsilon}^v) \mathbf{I} \right] + \bar{\omega}^{HS} \text{tr}(\boldsymbol{\varepsilon} - \boldsymbol{\varepsilon}^v) \mathbf{I} + O(\|\mathbf{H}\|^2),$$

where $\boldsymbol{\varepsilon} = 1/2(\mathbf{H} + \mathbf{H}^T)$, $\boldsymbol{\varepsilon}^v = 1/2(\mathbf{F}^v + \mathbf{F}^{vT} - 2\mathbf{I})$ is solution of the evolution equation

$$\begin{cases} \dot{\boldsymbol{\varepsilon}}^v(t) = \frac{\nu_m}{\eta_m} (\boldsymbol{\varepsilon} - \boldsymbol{\varepsilon}^v) \\ \boldsymbol{\varepsilon}^v(0) = \mathbf{0}, \end{cases}$$

and where we recall that the effective material constants $\bar{\mu}^{HS}$, $\bar{\kappa}^{HS}$, $\bar{\nu}^{HS}$, $\bar{\omega}^{HS}$ stand for the HS material constants (26). That is, the macroscopic response (56)–(57) reduces to the exact solution (27)–(28) for the case of isotropic suspensions with the iterative microstructure introduced in [13, 14]. As already pointed out in Remark 2, while not exact, it is therefore also very accurate for suspensions containing equiaxed vacuous bubbles at large.

Remark 6 (Finite deformations applied infinitesimally slowly and “infinitely” fast) In the limit of finite deformations that are applied either infinitesimally slowly or “infinitely” fast, following analogous steps to those outlined in Sect. 4, it is straightforward to show that the macroscopic response (56)–(57) reduces to (33) and (38), respectively. Again, these results are not exact in general, but they are very accurate for arbitrary deformations.

Remark 7 (The absence of storage of elastic energy) In the limit as $\mu_m = 0$ and $\nu_m \rightarrow +\infty$, when the underlying rubber matrix degenerates into a Newtonian fluid, a calculation akin to that presented in Sect. 5 shows that the macroscopic response (56)–(57), when written in terms of the macroscopic Cauchy stress $\mathbf{T} = J^{-1} \mathbf{S} \mathbf{F}^T$, specializes to

$$\mathbf{T}(t) = 2\bar{\eta}_{\kappa}^{HS} \mathbf{D} + \left(\bar{\eta}_{\mathcal{J}}^{HS} - \frac{2}{3} \bar{\eta}_{\kappa}^{HS} \right) \text{tr}(\mathbf{D}) \mathbf{I}, \tag{58}$$

where, again, $\mathbf{D} = \frac{1}{2}(\dot{\mathbf{F}}\mathbf{F}^{-1} + \mathbf{F}^{-T}\dot{\mathbf{F}}^T)$ and the effective material functions $\bar{\eta}_{\mathcal{K}}^{HS}$, $\bar{\eta}_{\mathcal{J}}^{HS}$ are given by the expressions (26). The constitutive response (58) is that of a *compressible non-Newtonian fluid* with deformation-dependent HS deviatoric viscosity $\bar{\eta}_{\mathcal{K}}^{HS}$ and HS volumetric viscosity $\bar{\eta}_{\mathcal{J}}^{HS}$. While the result (58) does not reduce to exact solution (43) in general, it does provide an accurate approximation for loading conditions along which the deformed bubbles remain isotropically distributed.

Remark 8 (Accuracy) By construction, as noted in the preceding three remarks, the proposed approximate macroscopic response (56)–(57) is either exact or very accurate for a broad spectrum of limiting loading and material-parameters regimes. Comparisons with a wide range of computational results, including those presented in Sect. 6 above, suggest that (56)–(57) remains accurate for arbitrary finite deformations, loading conditions, material constants μ_m, ν_m, η_m describing the viscoelastic behavior of the underlying rubber matrix, and characteristic functions θ_b describing the initial isotropic microstructure of the equiaxed bubbles.

8 Final Comments

Since the pioneering work of Sanchez-Palencia [22], Francfort and Suquet [23], and Suquet [7] in the 1980s, it is well known that even viscoelastic composite materials comprising constituents with the simplest types of short-range-memory (or narrow-spectrum) behaviors, after homogenization, turn out in general to feature long-range-memory (or broad-spectrum) behaviors.⁴ As noted by Ghosh et al. in [1], a special class of composite materials for which this daunting general rule does *not* apply are linear viscoelastic materials with a *single mechanism* of short-range relaxation. Indeed, after homogenization, such materials feature the same type of short-range-memory behavior as the local constituents. For convenience, we recall the demonstration here.

Consider, for direct comparison with the present work, an isotropic linear viscoelastic composite material characterized by the constitutive relation

$$\mathbf{S}(\mathbf{X}, t) = \int_{-\infty}^t \mathbf{L}(\mathbf{X}, t - \tau) \frac{\partial \mathbf{H}}{\partial \tau}(\mathbf{X}, \tau) d\tau \quad \text{with}$$

$$\mathbf{L}(\mathbf{X}, t) = 2\mu(\mathbf{X}) f(t)\mathcal{K} + 3\kappa(\mathbf{X}) f(t)\mathcal{J},$$

where, consistent with the notation employed in Sect. 3 above, $\mathbf{L}(\mathbf{X}, t)$ stands for the point-wise isotropic relaxation function. Although arbitrarily heterogeneous in space, this constitutive relation has a single mechanism of relaxation in time characterized by the function $f(t)$. Its Laplace transform is given by $\widehat{\mathbf{S}}(\mathbf{X}, s) = s \widehat{f}(s) [2\mu(\mathbf{X})\mathcal{K} + 3\kappa(\mathbf{X})\mathcal{J}] \widehat{\mathbf{H}}(\mathbf{X}, s)$. On substitution of this result in the governing equation $\text{Div} \widehat{\mathbf{S}}(\mathbf{X}, s) = \mathbf{0}$, it is plain that the s -dependent term $s \widehat{f}(s)$ can be factored out and hence that the governing equation reduces to $\text{Div}[(2\mu(\mathbf{X})\mathcal{K} + 3\kappa(\mathbf{X})\mathcal{J})\widehat{\mathbf{H}}(\mathbf{X}, s)] = \mathbf{0}$. It immediately follows that the resulting homogenized response (see Sect. 3) is given by a formula of the form

$$\mathbf{S}(t) = \int_{-\infty}^t \mathbf{L}(t - \tau) \frac{\partial \mathbf{H}}{\partial \tau}(\tau) d\tau \quad \text{with} \quad \mathbf{L}(t) = 2\tilde{\mu} f(t)\mathcal{K} + 3\tilde{\kappa} f(t)\mathcal{J}$$

⁴Precisely, by “short-range-memory” we mean viscoelastic behaviors that can be written in terms of a single internal variable, possibly tensorial, that is solution of a first-order ordinary differential equation in time. On the other hand, by “long-range-memory” we mean viscoelastic behaviors that are described by hereditary integrals which cannot be reduced to a single first-order ordinary differential equation.

and hence that it features the same single mechanism of relaxation as the local constituents. *Ergo*, when the single mechanism of relaxation of the local constituents is of short-range memory, the resulting homogenized behavior is also of short-range memory.

The above demonstration makes critical use of the Laplace transform and hence it applies only to *linear* viscoelastic composite materials. However, based on asymptotic and computational results for suspensions of rigid inclusions in rubber, Ghosh et al. [1] also conjectured that viscoelastic composite materials featuring a single mechanism of short-range relaxation, after homogenization, will continue to exhibit a single mechanism of short-range relaxation even when these are *nonlinear* and *finitely deformed*. In other words, the macroscopic response of such composite materials can be written in terms of a single macroscopic internal variable that is solution of a first-order ordinary differential equation in time.

The results presented throughout this work for suspensions of vacuous bubbles in rubber — a nonlinear and highly deformable material system with the shear relaxation of the underlying rubber matrix as its sole mechanism of relaxation — appear to be entirely consistent with the conjecture of Ghosh et al. [1].

We close by making explicit mention of two physically relevant generalizations of the present elementary study that merit future consideration. The first one has to do with accounting for non-Gaussian elasticity and nonlinear viscosity of the underlying rubber matrix. By now it is indeed well known from statistical mechanics and experiments alike that at sufficiently large deformations and deformation rates the elasticity of rubber is non-Gaussian and that its viscosity is nonlinear [34–40]. The second generalization involves accounting for the presence of both an internal pressure within the bubbles and of surface tension at the bubbles/rubber interfaces. By now it is also well established that even an internal bubble pressure as low as atmospheric pressure can have a significant effect on the response of suspensions of bubbles in soft rubbers [41, 42]. Equally well established is the fact that the presence of surface tension can become dominant for very small bubbles [43, 44]. These generalizations are expected to provide us with powerful tools to quantitatively understand a wide spectrum of phenomena, ranging from the effects of the undesirable presence of bubbles in many elastomers and elastomeric composites due to their fabrication process [48], to the response of seals in high-pressure gas tanks upon rapid decompression [49], to the hysteretic behavior of elastomeric syntactic foams [50].

Appendix: The Effective Volumetric Viscosity (55)

Assuming that the homogenized response (49) of the suspension depends on the macroscopic internal variable \mathbf{F}^v only through its symmetric combination $\mathbf{C}^v = \mathbf{F}^{vT} \mathbf{F}^v$ as does its local counterpart (8), it follows from material frame indifference and material symmetry that the effective volumetric viscosity $m_{\mathcal{J}}(\mathbf{F}, \mathbf{F}^v)$ admits the representation [45]

$$m_{\mathcal{J}}(\mathbf{F}, \mathbf{F}^v) = m_{\mathcal{J}}(I_1, I_2, I_3, I_1^v, I_2^v, I_3^v, I_4^v, I_5^v, I_6^v, I_7^v) \tag{59}$$

in terms of the ten standard invariants

$$\begin{aligned} I_1 &= \text{tr } \mathbf{C}, & I_2 &= \text{tr } \mathbf{C}^2, & I_3 &= \text{tr } \mathbf{C}^3, & I_1^v &= \text{tr } \mathbf{C}^v, & I_2^v &= \text{tr } \mathbf{C}^{v2}, \\ I_3^v &= \text{tr } \mathbf{C}^{v3}, & I_4^v &= \text{tr } (\mathbf{C}\mathbf{C}^v), & I_5^v &= \text{tr } (\mathbf{C}^2\mathbf{C}^v), & I_6^v &= \text{tr } (\mathbf{C}\mathbf{C}^{v2}), & I_7^v &= \text{tr } (\mathbf{C}^2\mathbf{C}^{v2}) \end{aligned} \tag{60}$$

of the macroscopic right Cauchy–Green deformation tensor \mathbf{C} and \mathbf{C}^v ; in order to keep the notational complexity to a minimum, since there is little risk of confusion, we make use of the same symbol $m_{\mathcal{J}}$ for functions of different arguments.

In principle, the precise form of (59) in terms of the ten invariants (60) can be deduced by generating computational results for the macroscopic response of the suspension of interest under suitable loading conditions that vary one of the ten invariants (60) at a time while keeping the other nine fixed and then having the proposed approximate macroscopic response (49) match those results thereby determining the corresponding effective volumetric viscosity (59). However, since the asymptotic and computational results in the main body of the text suggest that the nonlinearity of the effective volumetric viscosity $m_{\mathcal{J}}$ is dominated by the change in volume of the bubbles, as opposed to by their change in shape, we adopt a more pragmatic approach here and choose $J = \det \mathbf{F} = \sqrt{(I_1^3 - 3I_1 I_2 + 2I_3)/6}$ and $J^v = \det \mathbf{F}^v = \sqrt{(I_1^{v3} - 3I_1^v I_2^v + 2I_3^v)/6}$ as the sole two combinations of invariants (60) that $m_{\mathcal{J}}$ depends on. Accordingly, we write

$$m_{\mathcal{J}}(\mathbf{F}, \mathbf{F}^v) = m_{\mathcal{J}}(J, J^v). \tag{61}$$

Now, in order to deduce the precise form of (61), we consider the macroscopic response of a representative suspension under hydrostatic loading conditions wherein J and J^v are varied independently and then have the proposed approximate macroscopic response (56) with (57) match that result thereby determining the value of the effective viscosity $m_{\mathcal{J}}(J, J^v)$ as a function of its arguments. Precisely, consistent with the analogous result in elasticity (see Sects. 2.2 and 4 in [16]), we consider a suspension of bubbles with the so-called hollow-sphere-assemblage (*HS A*) microstructure [46]. As for the specific type of hydrostatic loading, we consider applied isotropic macroscopic deformation gradients of the form

$$\mathbf{F}(t) = J_0^{1/3} \mathbf{I} + \mathcal{H}(t) \left(J_1^{1/3} - J_0^{1/3} \right) \mathbf{I}, \tag{62}$$

where $\mathcal{H}(t)$ stands for the Heaviside function (35); this is a generalization of the loading (34) considered in Sect. 4.2 in that a macroscopic deformation gradient $\mathbf{F}_1 = J_1^{1/3} \mathbf{I}$ is applied infinitely fast starting from a state in equilibrium that is not necessarily undeformed but rather described by the macroscopic deformation gradient $\mathbf{F}_0 = J_0^{1/3} \mathbf{I}$. The macroscopic response of a suspension with the *HS A* microstructure under this type of loading condition can be worked out explicitly in the asymptotic limit as $t \rightarrow 0+$ from the analysis put forth in [47]. The result reads $\mathbf{S}^{HS A}(t) = \mathbf{P}^{HS A}(t) \mathbf{I}$ with

$$\begin{aligned} \mathbf{P}^{HS A}(t) = & \left(\frac{4J_1 + 1}{2J_1^{2/3}} - \frac{f_0^{1/3} J_1^{2/3} (4J_1 - 4 + 5f_0)}{2(J_1 + f_0 - 1)^{4/3}} \right) \mu_m \\ & + \left(\frac{J_0^{1/3} (4J_1 + J_0)}{2J_1^{2/3}} - \frac{J_1^{2/3} (J_0 + f_0 - 1)^{1/3} (4J_1 + J_0 + 5f_0 - 5)}{2(J_1 + f_0 - 1)^{4/3}} \right) \nu_m \\ & + \left[\frac{20J_1^3 - 10J_1^2 J_0 - 8J_1 J_0^2 - 5J_0^3}{J_1^{8/3} J_0^{1/3}} - \frac{1}{(J_1 + f_0 - 1)^{8/3} (J_0 + f_0 - 1)^{1/3}} \right. \\ & \times (3(1 - f_0)^3 - (1 - f_0)^2 (41J_0 - 32J_1) + (1 - f_0) (-50J_1^2 + 36J_1 J_0 + 23J_0^2) \\ & \left. + 20J_1^3 - 10J_1^2 J_0 - 8J_1 J_0^2 - 5J_0^3) \right] \frac{J_1^{2/3} \nu_m^2}{30\eta_m} t + O(t^2). \tag{63} \end{aligned}$$

Under the loading condition (62), the approximate macroscopic response (56)–(57) can also be written explicitly in the asymptotic limit as $t \rightarrow 0+$. The result reads $\mathbf{S}(t) = \mathbf{P}(t)\mathbf{I}$ with

$$\begin{aligned} \mathbf{P}(t) = & \left(\frac{4J_1 + 1}{2J_1^{2/3}} - \frac{f_0^{1/3} J_1^{2/3} (4J_1 - 4 + 5f_0)}{2(J_1 + f_0 - 1)^{4/3}} \right) \mu_m \\ & + \left(\frac{J_0^{1/3} (4J_1 + J_0)}{2J_1^{2/3}} - \frac{J_1^{2/3} (J_0 + f_0 - 1)^{1/3} (4J_1 + J_0 + 5f_0 - 5)}{2(J_1 + f_0 - 1)^{4/3}} \right) \nu_m \\ & - \left(\frac{J_1 + J_0}{J_1^{2/3} J_0^{2/3}} - \frac{J_1^{2/3} (J_1 + J_0 + 2f_0 - 2)}{(J_1 + f_0 - 1)^{4/3} (J_0 + f_0 - 1)^{2/3}} \right) \\ & \times \left(\frac{J_0^{1/3} (J_1 - 2J_0)}{J_1^{1/3}} - \frac{J_0 (J_1 - 2J_0 - f_0 + 1)}{(J_1 + f_0 - 1)^{1/3} (J_0 + f_0 - 1)^{2/3}} \right) \frac{2\nu_m^2}{3m_{\mathcal{J}}(J_1, J_0)} t \\ & + O(t^2). \end{aligned} \quad (64)$$

Matching (64) to (63) and exploiting the arbitrariness of J_0 and J_1 yields the effective volumetric viscosity (55).

Acknowledgements Support for this work by the National Science Foundation through the Grant CMMI-1901583.

References

1. Ghosh, K., Shrivali, B., Kumar, A., Lopez-Pamies, O.: The nonlinear viscoelastic response of suspensions of rigid inclusions in rubber: I — Gaussian rubber with constant viscosity. *J. Mech. Phys. Solids* **154**, 104544 (2021)
2. Halphen, B., Nguyen, Q.S.: Sur les matériaux standard généralisés. *J. Méc.* **14**, 39–63 (1975)
3. Ziegler, H., Wehrli, C.: The derivation of constitutive relations from the free energy and the dissipation function. *Adv. Appl. Mech.* **25**, 183–238 (1987)
4. Kumar, A., Lopez-Pamies, O.: On the two-potential constitutive modelling of rubber viscoelastic materials. *C. R., Méc.* **344**, 102–112 (2016)
5. Zener, C.M.: *Elasticity and Anelasticity of Metals*. University of Chicago Press, Chicago (1948)
6. Hill, R.: On constitutive macrovariables for heterogeneous solids at finite strain. *Proc. R. Soc. Lond. A* **326**, 131–147 (1972)
7. Suquet, P.: Elements of homogenization for inelastic solid mechanics. In: Sanchez-Palencia, E., Zaoui, A. (eds.) *Homogenization Techniques for Composite Media*. Lecture Notes in Physics, vol. 272, pp. 193–278. Springer, New York (1987)
8. Spinelli, S.A., Lefèvre, V., Lopez-Pamies, O.: Dielectric elastomer composites: a general closed-form solution in the small-deformation limit. *J. Mech. Phys. Solids* **83**, 263–284 (2015)
9. deBotton, G.: Transversely isotropic sequentially laminated composites in finite elasticity. *J. Mech. Phys. Solids* **53**, 1334–1361 (2005)
10. Francfort, G.A., Murat, F.: Homogenization and optimal bounds in linear elasticity. *Arch. Ration. Mech. Anal.* **94**, 307–334 (1986)
11. Idiart, M.I.: Modeling the macroscopic behavior of two-phase nonlinear composites by infinite-rank laminates. *J. Mech. Phys. Solids* **56**, 2599–2617 (2008)
12. Lopez-Pamies, O.: An exact result for the macroscopic response of particle-reinforced Neo-Hookean solids. *J. Appl. Mech.* **77**, 021016 (2010)
13. Lopez-Pamies, O., Idiart, M.I., Nakamura, T.: Cavitation in elastomeric solids: I — a defect-growth theory. *J. Mech. Phys. Solids* **59**, 1464–1487 (2011)
14. Lopez-Pamies, O., Nakamura, T., Idiart, M.I.: Cavitation in elastomeric solids: II — onset-of-cavitation surfaces for Neo-Hookean materials. *J. Mech. Phys. Solids* **59**, 1488–1505 (2011)
15. Hashin, Z., Shtrikman, S.: A variational approach to the theory of the elastic behaviour of multiphase materials. *J. Mech. Phys. Solids* **11**, 127–140 (1963)

16. Shriali, B., Lefèvre, V., Lopez-Pamies, O.: A simple explicit homogenization solution for the macroscopic elastic response of isotropic porous elastomers. *J. Mech. Phys. Solids* **122**, 364–380 (2019)
17. Michel, J.C., Lopez-Pamies, O., Ponte Castañeda, P., Triantafyllidis, N.: Microscopic and macroscopic instabilities in finitely strained porous elastomers. *J. Mech. Phys. Solids* **55**, 900–938 (2007)
18. Moraleta, J., Segurado, J., Llorca, J.: Finite deformation of porous elastomers: a computational micromechanics approach. *Philos. Mag.* **87**, 5607–5627 (2007)
19. Lopez-Pamies, O., Idiart, M.I.: An exact result for the macroscopic behavior of porous Neo-Hookean solids. *J. Elast.* **95**, 99–105 (2009)
20. Lefèvre, V., Garnica, A., Lopez-Pamies, O.: A WENO finite-difference scheme for a new class of Hamilton-Jacobi equations in nonlinear solid mechanics. *Comput. Methods Appl. Mech. Eng.* **349**, 17–44 (2019)
21. Hashin, Z.: Viscoelastic behavior of heterogeneous media. *J. Appl. Mech.* **32**, 630–636 (1965)
22. Sanchez-Palencia, E.: *Non Homogeneous Media and Vibration Theory*. Monograph in Physics, vol. 127. Springer, Berlin (1980)
23. Francfort, G.A., Suquet, P.: Homogenization and mechanical dissipation in thermoviscoelasticity. *Arch. Ration. Mech. Anal.* **96**, 265–293 (1986)
24. Taylor, G.I.: The viscosity of a fluid containing small drops of another fluid. *Proc. R. Soc. Lond. Ser. A* **138**, 41–48 (1932)
25. Acrivos, A.: The breakup of small drops and bubbles in shear flows. *Ann. N.Y. Acad. Sci.* **404**, 1–11 (1983)
26. Stone, H.A.: Dynamics of drop deformation and breakup in viscous fluids. *Annu. Rev. Fluid Mech.* **26**, 65–102 (1994)
27. Mader, H.M., Llewellyn, E.W., Mueller, S.P.: The rheology of two-phase magmas: a review and analysis. *J. Volcanol. Geotherm. Res.* **257**, 135–158 (2013)
28. Willis, J.R.: Variational and related methods for the overall properties of composites. *Adv. Appl. Mech.* **21**, 1–78 (1981)
29. Gusev, A.A.: Representative volume element size for elastic composites: a numerical study. *J. Mech. Phys. Solids* **45**, 1449–1459 (1997)
30. Michel, J.C., Moulinec, H., Suquet, P.: Effective properties of composite materials with periodic microstructure: a computational approach. *Comput. Methods Appl. Mech. Eng.* **172**, 109–143 (1999)
31. Segurado, J., Llorca, J.: A numerical approximation to the elastic properties of sphere-reinforced composites. *J. Mech. Phys. Solids* **50**, 2107–2121 (2002)
32. Ghossein, E., Lévesque, M.: A fully automated numerical tool for a comprehensive validation of homogenization models and its application to spherical particles reinforced composites. *Int. J. Solids Struct.* **49**, 1387–1398 (2012)
33. Lopez-Pamies, O., Goudarzi, T., Danas, K.: The nonlinear elastic response of suspensions of rigid inclusions in rubber: II — a simple explicit approximation for finite-concentration suspensions. *J. Mech. Phys. Solids* **61**, 19–37 (2013)
34. Treloar, L.R.G.: *The Physics of Rubber Elasticity*. Oxford University Press, Oxford (1975)
35. Doi, M., Edwards, S.F.: *The Theory of Polymer Dynamics*. Oxford University Press, New York (1998)
36. Gent, A.N.: Relaxation processes in vulcanized rubber. I. Relation among stress relaxation, creep, recovery, and hysteresis. *J. Appl. Polym. Sci.* **6**, 433–441 (1962)
37. Khan, A.S., Lopez-Pamies, O.: Time and temperature dependent response and relaxation of a soft polymer. *Int. J. Plast.* **18**, 1359–1372 (2002)
38. Amin, A.F.M.S., Lion, A., Sekita, S., Okui, Y.: Nonlinear dependence of viscosity in modeling the rate-dependent response of natural and high damping rubbers in compression and shear: experimental identification and numerical verification. *Int. J. Plast.* **22**, 1610–1657 (2006)
39. Lopez-Pamies, O.: A new I_1 -based hyperelastic model for rubber elastic materials. *C. R., Méc.* **338**, 3–11 (2010)
40. Chockalingam, S., Roth, C., Henzel, T., Cohen, T.: Probing local nonlinear viscoelastic properties in soft materials. *J. Mech. Phys. Solids* **146**, 104172 (2021)
41. Idiart, M.I., Lopez-Pamies, O.: On the overall response of elastomeric solids with pressurized cavities. *C. R., Méc.* **340**, 359–368 (2012)
42. Lopez-Pamies, O., Ponte Castañeda, P., Idiart, M.I.: Effects of internal pore pressure on closed-cell elastomeric foams. *Int. J. Solids Struct.* **49**, 2793–2798 (2012)
43. Gent, A.N., Tompkins, D.A.: Surface energy effects for small holes or particles in elastomers. *J. Polym. Sci. A-2 Polym. Phys.* **7**, 1483–1487 (1969)
44. Style, R., Boltynskiy, R., Allen, B., Jensen, K.E., Foote, H.P., Wettlaufer, J.S., Dufresne, E.R.: Stiffening solids with liquid inclusions. *Nat. Phys.* **11**, 82–87 (2015)
45. Boehler, J.P.: *Applications of Tensor Functions in Solid Mechanics*. Springer, Berlin (1987)

46. Hashin, Z.: Large isotropic elastic deformation of composites and porous media. *Int. J. Solids Struct.* **21**, 711–720 (1985)
47. Kumar, A., Aranda-Iglesias, D., Lopez-Pamies, O.: Some remarks on the effects of inertia and viscous dissipation in the onset of cavitation in rubber. *J. Elast.* **126**, 201–213 (2017)
48. Johnston, I.D., McCluskey, D.K., Tan, C.K.L., Tracey, M.C.: Mechanical characterization of bulk Sylgard 184 for microfluidics and microengineering. *J. Micromech. Microeng.* **24**, 035017 (2014)
49. Yamabe, J., Nishimura, S.: Influence of fillers on hydrogen penetration properties and blister fracture of rubber composites for O-ring exposed to highpressure hydrogen gas. *Int. J. Hydrog. Energy* **34**, 1977–1989 (2009)
50. Shrimali, B., Parnell, W.J., Lopez-Pamies, O.: A simple explicit model constructed from a homogenization solution for the large-strain mechanical response of elastomeric syntactic foams. *Int. J. Non-Linear Mech.* **126**, 103548 (2020)

Publisher's Note Springer Nature remains neutral with regard to jurisdictional claims in published maps and institutional affiliations.